SIAM J. NUMER. ANAL.
Vol. 54, No. 6, pp. 3332–3356
© 2016 Society for Industrial and Applied Mathematics

TWO FAMILIES OF $H(\mathrm{div})$ MIXED FINITE ELEMENTS ON QUADRILATERALS OF MINIMAL DIMENSION*

TODD ARBOGAST† AND MAICON R. CORREA‡

Abstract. We develop two families of mixed finite elements on quadrilateral meshes for approximating $(\mathbf{u}, p)$ solving a second order elliptic equation in mixed form. Standard Raviart–Thomas (RT) and Brezzi–Douglas–Marini (BDM) elements are defined on rectangles and extended to quadrilaterals using the Piola transform, which are well-known to lose optimal approximation of $\nabla \cdot \mathbf{u}$. Arnold–Boffi–Falk spaces rectify the problem by increasing the dimension of RT, so that approximation is maintained after Piola mapping. Our two families of finite elements are uniformly inf-sup stable, achieve optimal rates of convergence, and have minimal dimension. The elements for $\mathbf{u}$ are constructed from vector polynomials defined directly on the quadrilaterals, rather than being transformed from a reference rectangle by the Piola mapping, and then supplemented by two (one for the lowest order) basis functions that are Piola mapped. One family has full $H(\mathrm{div})$-approximation ($\mathbf{u}$, p, and $\nabla \cdot \mathbf{u}$ are approximated to the same order like RT) and the other has reduced $H(\mathrm{div})$-approximation (p and $\nabla \cdot \mathbf{u}$ are approximated to one less power like BDM). The two families are identical except for inclusion of a minimal set of vector and scalar polynomials needed for higher order approximation of $\nabla \cdot \mathbf{u}$ and p, and thereby we clarify and unify the treatment of finite element approximation between these two classes. The key result is a Helmholtz-like decomposition of vector polynomials, which explains precisely how a divergence is approximated locally. We develop an implementable local basis and present numerical results confirming the theory.

Key words. second order elliptic equation, mixed methods, divergence approximation, full $H(\mathrm{div})$-approximation, reduced $H(\mathrm{div})$-approximation, inf-sup stable

AMS subject classifications. 65N12, 65N30, 41A10

DOI. 10.1137/15M1013705

1. Introduction.

Let $\Omega \subset \mathbb{R}^2$ be a polygonal domain and consider the second order elliptic boundary value problem in mixed form

$$\mathbf{u} = -a\nabla p, \quad \nabla \cdot \mathbf{u} = f \quad \text{in } \Omega, \quad \mathbf{u} \cdot \nu = 0 \quad \text{on } \partial\Omega, \tag{1.1}$$

where $f \in L^2(\Omega)$, the tensor a is uniformly positive and bounded, and ν denotes the outer unit normal vector. We choose to treat homogeneous Neumann boundary conditions for simplicity; other conditions could be imposed. Let $H(\mathrm{div};\Omega) = \{\mathbf{v} \in (L^2(\Omega))^2 : \nabla \cdot \mathbf{u} \in L^2(\Omega)\}$. We expect that $\mathbf{u} \in \mathbf{V} = H(\mathrm{div};\Omega) \cap \{\mathbf{v} : \mathbf{v} \cdot \nu = 0 \text{ on } \partial\Omega\}$ and $p \in W = L^2(\Omega)/\mathbb{R}$. In mixed form, (1.1) is equivalent to the constrained minimization problem

$$\mathbf{u} = \operatorname*{arg\,min}_{\mathbf{v}\in\mathbf{V}, \nabla\cdot\mathbf{v}=f} \frac{1}{2}\|a^{-1/2}\mathbf{v}\|^2, \tag{1.2}$$

*Received by the editors March 24, 2015; accepted for publication (in revised form) August 5, 2016; published electronically November 22, 2016.

http://www.siam.org/journals/sinum/54-6/M101370.html

Funding: This work was supported by the U.S. National Science Foundation under grant DMS-1418752 and by the São Paulo Research Foundation (FAPESP) under grant 2013/19021-8.

†Department of Mathematics, University of Texas, Austin, TX 78712-1202, and Institute for Computational Engineering and Sciences, University of Texas, Austin, TX 78712-1229 (arbogast@ices.utexas.edu).

‡Instituto de Matemática Estatística e Computação Científica, Departamento de Matemática Aplicada, Universidade Estadual de Campinas, 651 Barão Geraldo, 13083-859, Campinas, SP, Brasil (maicon@ime.unicamp.br).

where $\|\cdot\|_\omega$ is the $L^2(\omega)$- or $(L^2(\omega))^2$-norm (here and elsewhere omit ω in the notation if it is Ω).

Let $(\cdot,\cdot)_\omega$ denote the $L^2(\omega)$ or $(L^2(\omega))^2$ inner-product. After multiplying (1.1) by test functions, integrating, and integrating one term by parts, or, equivalently, after introducing the Lagrange multiplier p and taking the derivative of (1.2), we obtain the weak or variational form: Find $(\mathbf{u}, p) \in \mathbf{V} \times W$ such that

$$(a^{-1}\mathbf{u}, \mathbf{v}) - (p, \nabla \cdot \mathbf{v}) = 0, \qquad \mathbf{v} \in \mathbf{V}, \tag{1.3}$$

$$(\nabla \cdot \mathbf{u}, w) = (f, w), \qquad w \in W. \tag{1.4}$$

Existence and uniqueness of the solution follows from the ellipticity (or coercivity) of the form $(a^{-1}\mathbf{u}, \mathbf{v})$ on the kernel of the divergence operator and the inf-sup condition [7, 13], which states that there is some $\gamma > 0$ such that

$$\inf_{w \in W} \sup_{\mathbf{v} \in \mathbf{V}} \frac{(w, \nabla \cdot \mathbf{v})}{\|w\| \|\mathbf{v}\|_{H(\mathrm{div})}} \geq \gamma > 0. \tag{1.5}$$

We use the notation $\|\cdot\|_{H(\mathrm{div};\omega)} = \{\|\cdot\|_\omega^2 + \|\nabla \cdot (\cdot)\|_\omega^2\}^{1/2}$ for the $H(\mathrm{div};\omega)$-norm. Later we will also need the norm $\|\cdot\|_{n,\omega}$ of the Sobolev space $H^n(\omega)$ of n times weakly differentiable functions in $L^2(\Omega)$.

Accurate and stable conforming finite element discretization of (1.3)–(1.4) requires inf-sup stable finite element spaces $\mathbf{V}_h \times W_h \subset \mathbf{V} \times W$ that are uniform in γ with respect to the finite element mesh parameters, such as the maximal element diameter h [26, 15, 27, 12, 9]. On meshes of triangles and rectangles, mixed finite element spaces normally satisfy the property that $\nabla \cdot \mathbf{V}_h = W_h$, and so p and $\nabla \cdot \mathbf{u}$ are approximated to the same order of accuracy. At least two classes of finite element spaces exist. The Raviart–Thomas (RT) elements of index $k \geq 0$ [26] approximate $\mathbf{u}$, p, and $\nabla \cdot \mathbf{u}$ to the same order $\mathcal{O}(h^{k+1})$, whereas Brezzi–Douglas–Marini (BDM) elements of index $k \geq 1$ [14] approximate $\mathbf{u}$ to order $\mathcal{O}(h^{k+1})$ but p and $\nabla \cdot \mathbf{u}$ to order $\mathcal{O}(h^k)$. We say that finite element spaces that satisfy the former properties are of the class of *full* $H(\mathrm{div})$*-approximation spaces*, and those of the other class are *reduced* $H(\mathrm{div})$*-approximation spaces*.

In this paper we consider approximation on quadrilateral finite element meshes. The RT and BDM elements are defined on rectangles and extended to quadrilaterals using the Piola transform [30, 26]. This creates a consistency error and loss of approximation of the divergence of the solution $\mathbf{u}$ [30, 15, 3, 9]. The Arnold–Boffi–Falk spaces (ABF) [3] rectify the problem by including more degrees of freedom in the space, so that approximation is maintained after Piola mapping.

Many papers address mixed finite element approximation on quadrilateral finite element meshes. We mention just three of them to illustrate some of the approaches used to overcome the difficulties. The work of Shen in the early 1990s [29, 28] covers only the lowest order elements, which are defined on a reference square and mapped via Piola. The approach is to use a "bubble function" (i.e., a vector function with zero normal trace on each edge) to modify the lowest order RT reference element so that the mapped element has constant divergence. Boffi, Kikuchi, and Schöberl [10] developed related $H(\mathrm{curl})$ finite elements for quadrilaterals by using a projection technique equivalent to reduced integration. Their approach obtained optimal order convergence of the eigenvalues of the Maxwell eigenvalue problem using first and second order elements. Bochev and Ridzal [8] reformulated the approximate mixed system (1.3)–(1.4) using ideas from mimetic finite difference methods. The reformulated method is actually algebraically identical to the original, but the interpretation

of the solution differs. In some sense, their method is a postprocessing of the lowest order RT solution that results in an optimal order approximation.

We present two new families of uniformly inf-sup stable finite element spaces that maintain optimal rates of convergence and have minimal dimension. Locally on an element, our spaces of index k have the dimension of exactly two (one if $k = 0$) more than the space of polynomials needed to obtain optimal approximation. Our finite elements are constructed from vector polynomials defined directly on the quadrilaterals rather than being transformed from a reference rectangle by the Piola mapping, and then supplemented by two (one if $k = 0$) basis functions that are Piola mapped. One family has full $H(\mathrm{div})$-approximation and the other has reduced $H(\mathrm{div})$-approximation. The two families are identical except for inclusion of a minimal set of vector polynomials in $\mathbf{V}_h$ and higher order polynomials in W_h that achieve approximation of the divergence and p to full order, and so in some sense we clarify and unify the treatment of finite element approximation between the two classes. The key result is a Helmholtz-like decomposition of vector polynomials (see Theorem 2.1), which explains precisely how a divergence is approximated locally by vector polynomials.

An outline of the paper follows. In the next section, we establish the Helmholtz-like decomposition and determine a set of sufficient conditions that a finite element space should satisfy to obtain stable, conforming, and optimal order full and reduced $H(\mathrm{div})$-approximation of the finite element method for (1.3)–(1.4). The conditions are finite element locality in $H(\mathrm{div})$, stability, and local and global consistency. In section 3 we recall the definition of the RT, BDM, and ABF spaces and define our new families of Arbogast-Correa (AC) spaces. In section 4, we give a detailed construction of the analogue of the RT π-projection operator [26] for AC spaces of any index. To do so, we need to define special linear polynomials tailored to the geometry of the given quadrilateral and also to define special vector polynomials. The difficulty is to verify that edge degrees of freedom (DOFs) can be set independently of divergence DOFs within our spaces and to identify the remaining DOFs. In section 5 we discuss practical implementation of the methods. We give an easily constructed basis for the full $H(\mathrm{div})$-approximation spaces and a constructible basis for the reduced spaces. Numerical results are presented in section 6 to verify the properties of the new spaces and contrast them with the existing spaces, up to index 2. Finally, we make some concluding remarks in the last section.

2. Conditions for mixed finite element spaces to be accurate and efficient. In this section, we state a set of conditions to be satisfied by a mixed finite element space that is sufficient to obtain accurate and efficient conforming approximation of (1.3)–(1.4).

We impose a conforming finite element mesh $\mathcal{T}_h$ of quadrilaterals over the domain Ω of maximal spacing h. We will assume that the mesh $\mathcal{T}_h$ is shape-regular, which ensures that the mesh does not degenerate to highly elongated or nearly triangular elements. The condition is that each element $E \in \mathcal{T}_h$ is uniformly shape-regular [22, pp. 104–105]. That is, E contains four (overlapping) triangles constructed from any choice of three vertices, and each such triangle has an inscribed circle, the minimal radius of which is ρ_E. If h_E denotes the diameter of E, the requirement is that the ratio $\rho_E/h_E \geq \sigma_* > 0$, where σ_* is independent of $\mathcal{T}_h$. We use the notation $h = \max_{E\in\mathcal{T}_h} h_E$, $|E|$ for the area of $E \in \mathcal{T}_h$, and $|e|$ for the length of a line segment e.

Let $\tilde{\mathbb{P}}_k = \mathrm{span}\{x^i y^{k-i} \,:\, i = 0, 1, \ldots, k\}$ be the homogeneous polynomials of exact degree $k \geq 0$, and let $\mathbb{P}_k = \bigoplus_{n=0}^{k} \tilde{\mathbb{P}}_n = \mathrm{span}\{x^i y^j \,:\, i, j = 0, 1, \ldots, k;\ i + j \leq k\}$ denote the space of polynomials of degree $k \geq 0$. Let $\mathbb{P}_{k_1,k_2} = \mathrm{span}\{x^i y^j \,:\, i =$

$0, 1, \ldots, k_1;\ j = 0, 1, \ldots, k_2\}$ be the space of polynomials of degree $k_1 \geq 0$ in $x = x_1$ and degree $k_2 \geq 0$ in $y = x_2$.

For $k \geq 0$, we will use the spaces of vector polynomials

$$\mathbf{x}\tilde{\mathbb{P}}_k = \begin{pmatrix} x \\ y \end{pmatrix} \tilde{\mathbb{P}}_k = \operatorname{span}\left\{ \begin{pmatrix} x^{i+1}y^{k-i} \\ x^i y^{k-i+1} \end{pmatrix} \,:\, i = 0, 1, \ldots, k \right\} \subset \tilde{\mathbb{P}}^2_{k+1}$$

and $\mathbf{x}\mathbb{P}_k = \bigoplus_{n=0}^{k} \mathbf{x}\tilde{\mathbb{P}}_n \subset \mathbb{P}^2_{k+1}$. Define the operator curl mapping scalars to vectors as $\operatorname{curl} w = (\frac{\partial w}{\partial y}, -\frac{\partial w}{\partial x})$. We also use the spaces

$$\operatorname{curl} \tilde{\mathbb{P}}_{k+1} = \operatorname{span}\left\{ \begin{pmatrix} (k+1-i)x^i y^{k-i} \\ -i x^{i-1} y^{k+1-i} \end{pmatrix} \,:\, i = 0, 1, \ldots, k+1 \right\} \subset \tilde{\mathbb{P}}^2_k$$

and $\operatorname{curl} \mathbb{P}_{k+1} = \bigoplus_{n=0}^{k} \operatorname{curl} \tilde{\mathbb{P}}_{n+1} \subset \mathbb{P}^2_k$.

2.1. A Helmholtz-like decomposition. The key to understanding mixed finite element space construction is to understand how a vector field is approximated in $H(\operatorname{div})$. In fact, the divergence operator induces a Helmholtz-like decomposition.

THEOREM 2.1. *For any $k \geq 0$, $\nabla \cdot \operatorname{curl} \tilde{\mathbb{P}}_{k+1} = 0$, $\nabla\cdot : \mathbf{x}\tilde{\mathbb{P}}_k \to \tilde{\mathbb{P}}_k$ is a one-to-one and onto map, and*

$$\tilde{\mathbb{P}}^2_k = \mathbf{x}\tilde{\mathbb{P}}_{k-1} \oplus \operatorname{curl} \tilde{\mathbb{P}}_{k+1} \quad \text{and} \quad \mathbb{P}^2_k = \mathbf{x}\mathbb{P}_{k-1} \oplus \operatorname{curl} \mathbb{P}_{k+1}. \tag{2.1}$$

Moreover, for every line e with normal vector ν_e, $\mathbf{x}\mathbb{P}_k \cdot \nu_e|_e \subset \mathbb{P}_k(e)$.

Proof. It is clear that $\nabla \cdot \operatorname{curl} \tilde{\mathbb{P}}_{k+1} = 0$. It is well-known that $\nabla \cdot (\mathbb{P}_k \oplus \mathbf{x}\tilde{\mathbb{P}}_k) = \mathbb{P}_k$ [26, 24, 19] (this property is contained in the commuting diagram for RT spaces on triangles). The homogeneous polynomials of degree k, $\tilde{\mathbb{P}}_k$, map from $\mathbf{x}\tilde{\mathbb{P}}_k$, and a dimension count shows that the map is one-to-one. It is also well-known that $\mathbf{x}\mathbb{P}_k \cdot \nu_e|_e \subset \mathbb{P}_k(e)$, since $\mathbf{x} \cdot \nu_e$ is a constant on the line e.

Finally, it is enough to show the first result in (2.1). Clearly $\tilde{\mathbb{P}}^2_k \supset \mathbf{x}\tilde{\mathbb{P}}_{k-1} + \operatorname{curl} \tilde{\mathbb{P}}_{k+1}$, and $\mathbf{x}\tilde{\mathbb{P}}_{k-1}$ and $\operatorname{curl} \tilde{\mathbb{P}}_{k+1}$ intersect at 0 (since their divergences differ). The dimensions lead us to the conclusion; that is, $\dim \tilde{\mathbb{P}}^2_k = 2(k+1)$ matches the sum of $\dim \mathbf{x}\tilde{\mathbb{P}}_{k-1} = k$ and $\dim \operatorname{curl} \tilde{\mathbb{P}}_{k+1} = k+2$. ∎

We conclude that the divergence of a vector field is approximated by vector polynomials to order $\mathcal{O}(h^k)$ *only* by those of the form $\mathbf{x}\mathbb{P}_{k-1}$.

2.2. Sufficient conditions. A family of mixed finite element spaces should satisfy three general conditions to be accurate and efficient. In general, every numerical method should be *consistent* and *stable.* Finite element methods use approximation spaces that are defined locally on each element $E \in \mathcal{T}_h$, and so a *locality* condition is also required. Consistency is rather subtle for mixed methods, so we split it into two conditions, *local consistency/approximability* and *global consistency.*

Let the finite element space index be k, where $k \geq 0$ for full and $k \geq 1$ for reduced $H(\operatorname{div})$-approximation. We require the following four conditions of the finite element space $\mathbf{V}_h \times W_h$, which restricts locally to $\mathbf{V}_h(E) \times W_h(E)$ on the element E, where either $E \in \mathcal{T}_h$ or E is the reference element $\hat{E} = [-1, 1]^2$.

2.2.1. Locality. The space $\mathbf{V}_h(E)$ is pieced together with neighboring elements to create the space $\mathbf{V}_h \subset H(\operatorname{div}; \Omega)$. In our context, we require the condition that $\mathbf{V}_h(E)$ will contain only vectors with normal components on the element edges being polynomials of degree k; that is, $\mathbf{V}_h(E) \cdot \nu|_e \subset \mathbb{P}_k(e)$ for each edge $e \subset \partial E$.

2.2.2. Stability. Unless one approximates naturally stable mixed systems [23] or uses unconditionally stabilized methods (see, e.g., [18]), one guarantees stability provided the discrete inf-sup condition (1.5) holds with γ independent of the finite element mesh parameters [7, 13, 26, 15, 27, 12, 9]. In this case, it is easy to establish from the finite element approximation of (1.3)–(1.4) the bound

$$\|\mathbf{u}_h\| + \|p_h\| \le C\|f\|.$$

The inf-sup condition essentially requires that $\nabla \cdot \mathbf{V}_h \supset W_h$. To attain stability of the divergence, i.e., the bound $\|\nabla \cdot \mathbf{u}_h\| \le C\|f\|$, one needs $\nabla \cdot \mathbf{V}_h \subset W_h$, so that $\nabla \cdot \mathbf{V}_h = W_h$.

2.2.3. Local consistency/approximability. For full $H(\mathrm{div})$-approximation elements (RT-style), to attain $\mathcal{O}(h^{k+1})$ accuracy for $\mathbf{u}$, p, and $\nabla \cdot \mathbf{u}$ requires (by Theorem 2.1) $\mathbf{V}_h(E) \supset \mathbb{P}_k^2 \oplus \mathbf{x}\tilde{\mathbb{P}}_k$ and $W_h(E) \supset \mathbb{P}_k$. For reduced $H(\mathrm{div})$-approximation elements (BDM-style), to attain $\mathcal{O}(h^{k+1})$ accuracy for $\mathbf{u}$ but only $\mathcal{O}(h^k)$ for p and $\nabla \cdot \mathbf{u}$ requires $\mathbf{V}_h(E) \supset \mathbb{P}_k^2$ and $W_h(E) \supset \mathbb{P}_{k-1}$.

Shape-regularity and the Bramble–Hilbert [11] or the Dupont–Scott [20] lemma then give accurate approximation within the finite element space (by, e.g., taking the L^2-projections), i.e., there is a constant $C > 0$ such that for all $\mathcal{T}_h$ and $E \in \mathcal{T}_h$,

$$\inf_{\mathbf{v}_h \in \mathbf{V}_h(E)} \|\mathbf{u} - \mathbf{v}_h\|_E \le C\|\mathbf{u}\|_{j,E} h_E^j, \qquad j = 0, 1, \ldots, k+1, \tag{2.2}$$

$$\inf_{\mathbf{v}_h \in \mathbf{V}_h(E)} \|\nabla \cdot (\mathbf{u} - \mathbf{v}_h)\|_E \le C\|\nabla \cdot \mathbf{u}\|_{j,E} h_E^j, \quad j = 0, 1, \ldots, \ell+1, \tag{2.3}$$

$$\inf_{w_h \in W_h(E)} \|p - w_h\|_E \le C\|p\|_{j,E} h_E^j, \qquad j = 0, 1, \ldots, \ell+1, \tag{2.4}$$

where $\ell = k \ge 0$ and $\ell = k - 1 \ge 0$ for full and reduced $H(\mathrm{div})$-approximation, respectively.

2.2.4. Global consistency: The π-projection operator. A global consistency condition is required to properly handle the divergence constraint (1.4). The primary families of mixed finite spaces achieve global consistency by requiring that $\nabla \cdot \mathbf{V}_h = W_h$ (or that this holds locally on reference elements $\hat{E}$) and that there exists a projection operator π defined for $\mathbf{v} \in H(\mathrm{div}; \Omega) \cap (L^{2+\epsilon}(\Omega))^2$, $\epsilon > 0$, with $\pi\mathbf{v} \in \mathbf{V}_h$ satisfying three properties. First, the operator π is pieced together from locally defined operators π_E. Second, π satisfies the commuting diagram property [19], which is that $\mathcal{P}_{W_h} \nabla \cdot \mathbf{v} = \nabla \cdot \pi\mathbf{v}$, where $\mathcal{P}_{W_h}$ is the L^2-orthogonal projection operator onto W_h. Finally, π_E is bounded in, say, H^1, so that the approximation results (2.2)–(2.3) hold for $\mathbf{v}_h = \pi\mathbf{u}$, with now $j \ge 1$ in (2.2) [20, 15, 17, 9]. Note also that now (2.3) holds over the full space $\mathbf{V}_h$.

If π exists, then there is a vector $\pi\mathbf{u} \in \mathbf{V}_h$ quasi-optimally close to $\mathbf{u}$ that satisfies $\nabla \cdot \pi\mathbf{u} = \mathcal{P}_{W_h} f$, which is the discrete form of the divergence constraint (1.4). This shows global consistency between the minimization problem (1.2) and the finite element space $\mathbf{V}_h \times W_h$, i.e., the finite element method can consistently set the divergence constraint.

It is well-known that the existence of π simplifies our four conditions. First, the local approximation condition (2.3) follows from (2.4) and the commuting diagram property. Second, stability, i.e., the discrete inf-sup condition (1.5), holds. To review the argument, we require a vector $\mathbf{v} \in H^1$ such that $\nabla \cdot \mathbf{v} = w_h \in W_h$ and $\|\mathbf{v}\|_1 \le C_1\|w_h\|$ for some constant $C_1 > 0$ (see, e.g., [6] for a construction). Then $\|\pi\mathbf{v}\| \le$

$\|\mathbf{v}\| + \|\mathbf{v} - \pi\mathbf{v}\| \le \|\mathbf{v}\| + C_2 h\|\mathbf{v}\|_1 \le C_3\|w_h\|$ using (2.2), and so

$$\sup_{\mathbf{v}_h \in \mathbf{V}_h} \frac{(w_h, \nabla\cdot\mathbf{v}_h)}{\|\mathbf{v}_h\|_{H(\mathrm{div})}} \ge \frac{(w_h, \nabla\cdot\pi\mathbf{v})}{\|\pi\mathbf{v}\|_{H(\mathrm{div})}} = \frac{\|w_h\|^2}{\{\|\pi\mathbf{v}\|^2 + \|w_h\|^2\}^{1/2}} \ge \frac{\|w_h\|}{\sqrt{C_3^2+1}}. \tag{2.5}$$

2.3. Error analysis. For completeness, we briefly review the known error analysis of finite element approximation of (1.3)–(1.4) using a space $\mathbf{V}_h \times W_h$ satisfying only our four conditions. The equations for the error are

$$(a^{-1}(\mathbf{u} - \mathbf{u}_h), \mathbf{v}_h) - (p - p_h, \nabla\cdot\mathbf{v}_h) = 0, \quad \mathbf{v}_h \in \mathbf{V}_h, \tag{2.6}$$

$$(\nabla\cdot(\mathbf{u} - \mathbf{u}_h), w_h) = 0, \quad w_w \in W_h. \tag{2.7}$$

Since $\nabla\cdot\mathbf{V}_h = W_h$, we can replace p by $\mathcal{P}_{W_h}p$, and since $\nabla\cdot\pi\mathbf{u} = \mathcal{P}_{W_h}\nabla\cdot\mathbf{u}$, we can replace $\nabla\cdot\mathbf{u}$ by $\nabla\cdot\pi\mathbf{u}$. Substitute $\mathbf{v}_h = \pi\mathbf{u} - \mathbf{u}_h \in \mathbf{V}_h$ and $w_h = \mathcal{P}_{W_h}p - p_h + \nabla\cdot(\pi\mathbf{u} - \mathbf{u}_h) \in W_h$, and add the equations. Two terms cancel identically (without global consistency, these two terms would be troublesome and lead to a loss of accuracy in the estimate). The result is

$$(a^{-1}(\mathbf{u} - \mathbf{u}_h), \mathbf{u} - \mathbf{u}_h) + \|\nabla\cdot(\pi\mathbf{u} - \mathbf{u}_h)\|^2 = (a^{-1}(\mathbf{u} - \mathbf{u}_h), \mathbf{u} - \pi\mathbf{u}). \tag{2.8}$$

The inf-sup condition (2.5) and (2.6) show that

$$\|\mathcal{P}_{W_h}p - p_h\| \le C\|\mathbf{u} - \mathbf{u}_h\|, \tag{2.9}$$

and so we have the optimal error estimates

$$\|\mathbf{u} - \mathbf{u}_h\| + \|\nabla\cdot(\pi\mathbf{u} - \mathbf{u}_h)\| + \|\mathcal{P}_{W_h}p - p_h\| \le C\|\mathbf{u}\|_j h^j, \quad j = 1, 2, \ldots, k+1. \tag{2.10}$$

The projections can be removed for full $H(\mathrm{div})$-approximation spaces, but for reduced spaces, a single power of h is lost for approximation of $\nabla\cdot\mathbf{u}$ and p.

3. Families of mixed finite element spaces on quadrilaterals. Before presenting our new families of finite element spaces minimally meeting the four conditions of section 2.2, we review the three most related existing spaces.

3.1. Classic RT and BDM spaces on rectangles. The RT finite element space of index $k \ge 0$ (RT_k) is a full $H(\mathrm{div})$-approximation space [26, 15, 27, 9]. It is defined on a rectangular element $R \in \mathcal{T}_h$ as

$$\mathbf{V}^k_{\mathrm{RT}}(R) = \mathbb{P}_{k+1,k} \times \mathbb{P}_{k,k+1} \quad \text{and} \quad W^k_{\mathrm{RT}}(R) = \mathbb{P}_{k,k}. \tag{3.1}$$

The BDM space of index $k \ge 1$ (BDM_k) is a reduced $H(\mathrm{div})$-approximation space [14], and it is defined on rectangle $R \in \mathcal{T}_h$ as

$$\mathbf{V}^k_{\mathrm{BDM}}(R) = (\mathbb{P}_k)^2 \oplus \mathrm{span}\{\mathrm{curl}(x^{k+1}y), \mathrm{curl}(xy^{k+1})\} \text{ and } W^k_{\mathrm{BDM}}(R) = \mathbb{P}_{k-1}. \tag{3.2}$$

Both spaces have the properties that $\nabla\cdot\mathbf{V}(R) = W(R)$ and $\mathbf{V}(R)\cdot\nu|_e \subset \mathbb{P}_k(e)$ for each edge e of ∂R. In fact, it is well-known that they both satisfy the conditions of section 2.2, including the existence of the π projection operators.

3.2. Piola mapping to quadrilaterals. Extension of the RT and BDM spaces to quadrilaterals is accomplished via the Piola transformation [30, 26]. Fix the reference element $\hat{E} = [-1, 1]^2$ and take any quadrilateral $E \in \mathcal{T}_h$ with corner vertices $\mathbf{x}^i_c$,

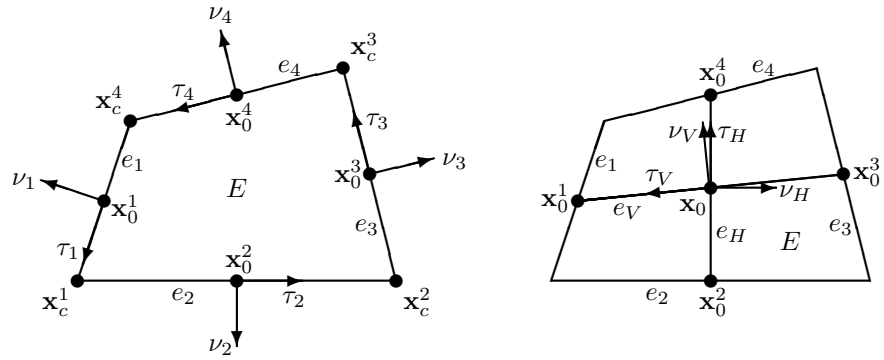

FIG. 1. *A counterclockwise oriented convex quadrilateral E with edges e_i, midpoints $\mathbf{x}_0^i$, outer unit normals ν_i, unit tangents τ_i (oriented by the right-hand rule from ν_i), and vertex "corners" $\mathbf{x}_c^i$ labeled in the direction of τ_i from $\mathbf{x}_0^i$, for $i = 1, 2, 3, 4$. Also depicted are the lines joining opposite midpoints, for which the line from $\mathbf{x}_0^2$ to $\mathbf{x}_0^4$, e_H, has unit "horizontal" normal ν_H pointing toward e_3 and unit tangent τ_H. Also shown are these quantities for the line e_V from $\mathbf{x}_0^3$ to $\mathbf{x}_0^1$, i.e., "vertical" unit normal ν_V pointing toward e_4 and unit tangent τ_V.*

$i = 1, 2, 3, 4$, oriented counterclockwise around ∂E (see Figure 1). Define the bijective and bilinear map $\mathbf{F}_E : \hat{E} \to E$ as

$$\mathbf{F}_E(\hat{\mathbf{x}}) = \mathbf{F}_E(\hat{x}, \hat{y}) = \frac{1}{4}\big\{\mathbf{x}_c^1(1-\hat{x})(1-\hat{y}) + \mathbf{x}_c^2(1+\hat{x})(1-\hat{y}) + \mathbf{x}_c^3(1+\hat{x})(1+\hat{y}) + \mathbf{x}_c^4(1-\hat{x})(1+\hat{y})\big\}. \tag{3.3}$$

Let $D\mathbf{F}_E(\hat{\mathbf{x}})$ denote the Jacobian matrix and $J_E(\hat{\mathbf{x}}) = \det(D\mathbf{F}_E(\hat{\mathbf{x}}))$. The Piola transform $\mathcal{P}_E$ maps a vector $\hat{\mathbf{v}} : \hat{E} \to \mathbb{R}^2$ to a vector $\mathbf{v} : E \to \mathbb{R}^2$ by the formula

$$\mathbf{v}(\mathbf{x}) = \mathcal{P}_E(\hat{\mathbf{v}})(\mathbf{x}) = \frac{1}{J_E} D\mathbf{F}_E \hat{\mathbf{v}}(\hat{\mathbf{x}}), \quad \text{where } \mathbf{x} = \mathbf{F}_E(\hat{\mathbf{x}}). \tag{3.4}$$

For a scalar function w, we define the map $\hat{w}$ by $\hat{w}(\hat{\mathbf{x}}) = w(\mathbf{x})$, where again $\mathbf{x} = \mathbf{F}_E(\hat{\mathbf{x}})$. The Piola transform preserves the divergence and normal components of $\hat{\mathbf{v}}$ in the sense that

$$(\hat{\nabla} \cdot \hat{\mathbf{v}}, \hat{w})_{\hat{E}} = (\nabla \cdot \mathbf{v}, w)_E \quad \forall\, w, \tag{3.5}$$

$$(\hat{\mathbf{v}} \cdot \hat{\nu}, \hat{\mu})_{\hat{e}} = (\mathbf{v} \cdot \nu, \mu)_e \quad \forall\, \mu \text{ and each edge } e \subset \partial E,\ e = \mathbf{F}_E(\hat{e}). \tag{3.6}$$

Because the normal components are preserved, one can piece together a conforming finite element space from the local spaces defined by Piola mapping the RT and BDM spaces on rectangles. That is, the RT finite element space of index $k \geq 0$ (RT_k) is defined on a quadrilateral element $E \in \mathcal{T}_h$ as

$$\mathbf{V}_{\mathrm{RT}}^k(E) = \mathcal{P}_E(\mathbb{P}_{k+1,k} \times \mathbb{P}_{k,k+1}) \quad \text{and} \quad W_{\mathrm{RT}}^k(E) = \mathbb{P}_{k,k} \circ \mathbf{F}_E^{-1}, \tag{3.7}$$

and the BDM element of index $k \geq 1$ (BDM_k) is defined as

$$\mathbf{V}_{\mathrm{BDM}}^k(E) = \mathcal{P}_E\big((\mathbb{P}_k)^2 \oplus \mathrm{span}\big\{\mathrm{curl}(x^{k+1}y), \mathrm{curl}(xy^{k+1})\big\}\big) \quad \text{and} \quad W_{\mathrm{BDM}}^k(E) = \mathbb{P}_{k-1} \circ \mathbf{F}_E^{-1}. \tag{3.8}$$

The problem with these spaces is well-known [30, 15, 3, 9]. Since $\mathbf{F}_E$ is bilinear, rather than affine, the Jacobian $J_E(\mathbf{x})$ is a linear function, and so the finite element functions $\mathbf{v}_h$ are rational functions rather than polynomials. This leads to a loss of global consistency ($\nabla \cdot \mathbf{V}_h \neq W_h$), and therefore a loss of convergence for $\nabla \cdot \mathbf{u}_h$ for RT elements and even worse convergence for BDM elements.

3.3. ABF spaces on quadrilaterals. The ABF spaces [3] rectify the problems with the RT and BDM spaces. However, the ABF spaces are also defined on quadrilaterals by Piola mapping from vectors defined on the reference square $\hat{E} = [-1, 1]^2$.

Replacing our global consistency condition is a general theoretical result [3] that Piola mapped vectors from a square $\hat{E}$ to a shape-regular but otherwise arbitrary quadrilateral $E \in \mathcal{T}_h$ are accurate to order $o(h^k)$ for $\mathbf{u}$ if and only if

$$\hat{\mathbf{V}}(\hat{E}) \supset \mathbf{S}_k = (\mathbb{P}_{k+1,k} \times \mathbb{P}_{k,k+1}) \cap \mathbb{P}_{2k}^2 \oplus \operatorname{span}\{(\hat{x}^{k+1}\hat{y}^k, -\hat{x}^k\hat{y}^{k+1})\},$$

and $o(h^k)$ for $\nabla \cdot \mathbf{u}$ if and only if

$$\hat{\nabla} \cdot \hat{\mathbf{V}}(\hat{E}) \supset R_k = \mathbb{P}_{k+1,k+1} \cap \mathbb{P}_{2k+1}.$$

For a full $H(\mathrm{div})$-approximation element, the minimal local space of index $k \geq 0$ is

$$\hat{\mathbf{V}}^k_{\mathrm{ABF}}(\hat{E}) = \mathbb{P}_{k+2,k} \times \mathbb{P}_{k,k+2} \quad \text{and} \quad \hat{W}^k_{\mathrm{ABF}}(\hat{E}) = \mathbb{P}_{k+1,k+1} \cap \mathbb{P}_{2k+1}. \tag{3.9}$$

Note that $\hat{W}^k_{\mathrm{ABF}}(\hat{E}) = \hat{\nabla}\cdot\hat{\mathbf{V}}^k_{\mathrm{ABF}}(\hat{E}) = R_k$ and that $\hat{\mathbf{V}}^k_{\mathrm{ABF}}(\hat{E}) \cdot \nu|_{\hat{e}} \subset \mathbb{P}_k(\hat{e})$ for every edge $\hat{e} \subset \partial\hat{E}$. The four conditions of section 2.2 hold on $\hat{E}$, including the existence of the $\hat{\pi}$ operator.

The ABF space of index $k \geq 0$ on $E \in \mathcal{T}_h$ is then defined as

$$\mathbf{V}^k_{\mathrm{ABF}}(E) = \mathcal{P}_E(\mathbb{P}_{k+2,k} \times \mathbb{P}_{k,k+2}) \text{ and } W^k_{\mathrm{ABF}}(E) = (\mathbb{P}_{k+1,k+1} \cap \mathbb{P}_{2k+1}) \circ \mathbf{F}_E^{-1}. \tag{3.10}$$

These spaces have the advantage over RT spaces in that their performance is independent of the quadrilateral distortion (subject only to shape-regularity) by the theoretical result noted above. This advantage comes at the expense of incorporating many extra degrees of freedom needed to maintain accuracy after mapping via Piola (i.e., to maintain a type of global consistency *after* the Piola mapping).

3.4. Two new families: AC spaces on quadrilaterals. We apply the conditions of section 2.2 in a minimal way to construct our new spaces. The goal is to apply the conditions over E, not over the reference $\hat{E}$. That is, the vectors we will use are vector polynomials over the element E, not vector rational functions mapped from vector polynomials on $\hat{E}$. That this goal by itself is an impossibility is seen in the BDM spaces on rectangles. For $\mathbf{V}^k_{\mathrm{BDM}}(R)$, one includes two polynomials of higher degree $k+1$ which nonetheless retain normal components of degree k. There is no such polynomial on general quadrilaterals E. Instead, we will achieve our goal up to addition of two vectors that are Piola mapped from $\hat{E}$ (actually only one for index $k = 0$).

To avoid difficulties, these supplemental vectors will have no divergence, and their normal components will be polynomials of degree k. We will make a specific choice later of vector polynomials on the reference element $\hat{E}$, but for now they must lie in

$$\hat{\sigma}^k_i \subset \operatorname{curl}\left(\mathbb{P}_{k+1} \oplus \operatorname{span}\{\hat{x}^{k+1}\hat{y}, \hat{x}^k\hat{y}^2, \ldots, \hat{x}\hat{y}^{k+1}\}\right), \quad i = 1, 2, \tag{3.11}$$

and then the space of supplemental vectors is

$$\mathbb{S}_k = \operatorname{span}\{\sigma^k_1, \sigma^k_2\}, \quad \text{where} \quad \sigma^k_i = \mathcal{P}_E\hat{\sigma}^k_i, \quad i = 1, 2. \tag{3.12}$$

For $E \in \mathcal{T}_h$ and index $k \geq 0$, our new full $H(\mathrm{div})$-approximation space is defined locally as

$$\mathbf{V}_{\mathrm{AC}}^k(\mathbb{S}_k, E) = \mathbb{P}_k^2 \oplus \mathbf{x}\tilde{\mathbb{P}}_k \oplus \mathbb{S}_k \qquad \text{and} \quad W_{\mathrm{AC}}^k(E) = \mathbb{P}_k. \tag{3.13}$$

For index $k \geq 1$, our new reduced $H(\mathrm{div})$-approximation space is defined locally as

$$\mathbf{V}_{\mathrm{AC}}^{k,\mathrm{red}}(\mathbb{S}_k, E) = \mathbb{P}_k^2 \oplus \mathbb{S}_k \qquad \text{and} \quad W_{\mathrm{AC}}^{k,\mathrm{red}}(E) = \mathbb{P}_{k-1}. \tag{3.14}$$

These spaces satisfy the locality and local consistency/approximability conditions of section 2.2. They can be pieced together to form the global spaces $\mathbf{V}_{\mathrm{AC}}^k(\mathbb{S}_k) \times W_{\mathrm{AC}}^k$ and $\mathbf{V}_{\mathrm{AC}}^{k,\mathrm{red}}(\mathbb{S}_k) \times W_{\mathrm{AC}}^{k,\mathrm{red}}$. As we will show in Theorem 4.5, they are finite element spaces of minimal dimension consistent with the desired locality and polynomial approximation conditions. The spaces also unify the notion of full and reduced $H(\mathrm{div})$-approximations, since from the reduced spaces, one merely includes $\mathbf{x}\tilde{\mathbb{P}}_k$ in $\mathbf{V}_h(E)$ and $\tilde{\mathbb{P}}_k$ in $W_h(E)$ if one wishes full approximation.

It remains to show the global consistency condition in the form of the existence of a π operator, which will also give the stability condition.

We believe that a wide range of choices can be made for the supplementary functions. We require $\hat{\sigma}_1^k$ to have a nontrivial component of $\mathrm{curl}(\hat{x}^{k+1}\hat{y})$ and $\hat{\sigma}_2^k$ to have a nontrivial component of $\mathrm{curl}(\hat{x}\hat{y}^{k+1})$, and we require that these are linearly independent for $k \neq 0$. Then $\hat{\sigma}_i \notin \mathbb{P}_k^2 \oplus \mathbf{x}\tilde{\mathbb{P}}_k$ and the functions are truly supplements even on elements affine equivalent to $\hat{E}$. However, we only show the construction of π_E on a general quadrilateral using the choice

$$\begin{cases} \hat{\sigma}_1^k = \mathrm{curl}(\hat{x}^{k-1}(1-\hat{x}^2)\hat{y}) \quad \text{and} \quad \hat{\sigma}_2^k = \mathrm{curl}(\hat{x}\hat{y}^{k-1}(1-\hat{y}^2)), & k \geq 1, \\ \hat{\sigma}^0 = \mathrm{curl}(\hat{x}\hat{y}), & k = 0. \end{cases} \tag{3.15}$$

For this choice, the construction of π will be demonstrated in section 4. Other choices could be used, provided that one verifies that a *constant divergence edge basis* can be constructed for each quadrilateral E (see section 4 for the meaning and the details).

3.5. A comparison of the spaces. It is well-known that in dimension two, $\dim \mathbb{P}_n = \frac{1}{2}(n+2)(n+1)$, $\dim \tilde{\mathbb{P}}_n = n+1$, and $\dim \mathbb{P}_{n_1,n_2} = (n_1+1)(n_2+1)$. A comparison of the dimensions of full and reduced $H(\mathrm{div})$-approximation spaces appears in Table 1. Our new spaces are of minimal total dimension subject to the locality conditions and local consistency/approximability. The RT, BDM, and ABF spaces are defined on rectangles and extended to general quadrilaterals using the Piola transformation. The RT and BDM spaces lose accuracy on general quadrilaterals, and so these should be considered as applying only to rectangular meshes.

Our new family of reduced $H(\mathrm{div})$-approximation spaces are the same as BDM on rectangles but differ on quadrilaterals. Our family of full $H(\mathrm{div})$-approximation spaces $\mathbf{V}_{\mathrm{AC}}^k$ appear to be new even on rectangular meshes, except that on rectangles, AC_0 is the same as RT_0.

4. Construction of the π operators for the AC spaces. In this section we construct the π-operators discussed in section 2.2.4 for the reduced and full $H(\mathrm{div})$-approximation spaces $\mathbf{V}_{\mathrm{AC}}^{k,\mathrm{red}} \times W_{\mathrm{AC}}^{k,\mathrm{red}}$ and $\mathbf{V}_{\mathrm{AC}}^k \times W_{\mathrm{AC}}^k$, i.e., the projection operators $\pi^{\mathrm{red}} : H(\mathrm{div}) \cap (L^{2+\epsilon}(\Omega))^2 \to \mathbf{V}_{\mathrm{AC}}^{k,\mathrm{red}}$ and $\pi : H(\mathrm{div}) \cap (L^{2+\epsilon}(\Omega))^2 \to \mathbf{V}_{\mathrm{AC}}^k$. As in the

TABLE 1

A comparison of the dimensions of the local RT, ABF, BDM, and AC spaces on quadrilateral E. BDM spaces coincide with AC spaces on rectangles, and they have the same local dimension. RT, BDM, and ABF spaces are defined on rectangles and extended to general quadrilaterals using the Piola transformation. Only the ABF and AC spaces give optimal convergence on quadrilaterals.

	RT_k	ABF_k	AC_k	BDM, $\mathrm{AC}_k^{\mathrm{red}}$
Approx.	Full	Full	Full	Reduced
$\dim \mathbf{V}(E)$	$2(k+2)(k+1)$	$2(k+3)(k+1)$	$(k+3)(k+1)$ $+2$ ($+1$ if $k=0$)	$(k+2)(k+1)$ $+2$
$\dim W(E)$	$(k+1)^2$	$(k+2)^2-1$	$\frac{1}{2}(k+2)(k+1)$	$\frac{1}{2}(k+1)k$
$k=0$	$4+1$	$6+3$	$4+1$	——
$k=1$	$12+4$	$16+8$	$10+3$	$8+1$
$k=2$	$24+9$	$30+15$	$17+6$	$14+3$

case of BDM spaces, our operators are defined locally on each $E \in \mathcal{T}_h$. For $\mathbf{u}$, we define $\pi_E^{\mathrm{red}}\mathbf{u}$ in terms of the DOFs

$$(\mathbf{u}\cdot\nu,\mu)_e \quad \forall\, \mu \in \mathbb{P}_k(e) \text{ for each edge } e \subset \partial E, \tag{4.1}$$

$$(\mathbf{u},\nabla w)_E \quad \forall\, w \in \mathbb{P}_{k-1}, \tag{4.2}$$

$$(\mathbf{u},\mathbf{v})_E \quad \forall\, \mathbf{v} \in \mathbb{B}_k \subset \mathbb{P}_k^2, \tag{4.3}$$

where $\mathbb{B}_k$ is defined later in (4.45). For $\pi_E\mathbf{u}$, we add the DOFs

$$(\mathbf{u},\nabla w)_E \quad \forall\, w \in \tilde{\mathbb{P}}_k. \tag{4.4}$$

If they exist, these operators satisfy all the required properties. The local versions can be pieced together to form π^{red} and π on the entire space because of (4.1). The commuting diagram property is easy to prove. For the reduced spaces, let $w_h \in W_{\mathrm{AC}}^{k,\mathrm{red}}(E) = \mathbb{P}_{k-1}$. Then DOFs (4.1)–(4.2) imply

$$\begin{aligned}(\nabla\cdot\mathbf{u},w_h)_E &= -(\mathbf{u},\nabla w_h)_E + (\mathbf{u}\cdot\nu,w_h)_{\partial E}\\ &= -(\pi_E^{\mathrm{red}}\mathbf{u},\nabla w_h)_E + (\pi_E^{\mathrm{red}}\mathbf{u}\cdot\nu,w_h)_{\partial E} = (\nabla\cdot\pi_E^{\mathrm{red}}\mathbf{u},w_h)_E,\end{aligned}$$

which is the required property for π_E^{red}. Similarly π_E satisfies the property, since then $w_h \in W_{\mathrm{AC}}^k(E) = \mathbb{P}_k = \mathbb{P}_{k-1} \oplus \tilde{\mathbb{P}}_k$ and we added DOFs (4.4). Finally, the operators are clearly bounded in $H^1(\Omega)$.

To prove existence of π_E^{red} and π_E, we need to show that the dimensions of the local spaces match the number of DOFs and unisolvence of the DOFs. We will see later that $\dim \mathbb{B}_k = \dim \mathbb{P}_{k-3}$, so when $k \geq 1$, the number of reduced DOFs is

$$\begin{aligned}&4\dim\mathbb{P}_k(e) + \dim\mathbb{P}_{k-1} - 1 + \dim\mathbb{B}_k = 4(k+1) + \tfrac{1}{2}(k+1)k - 1 + \tfrac{1}{2}(k-1)(k-2)\\ &\quad = k^2+3k+4 = (k+2)(k+1)+2 = \dim\mathbb{P}_k^2 + 2 = \dim\mathbf{V}_{\mathrm{AC}}^{k,\mathrm{red}},\end{aligned}$$

and the number of full DOFs is

$$k^2+3k+4+\dim\tilde{\mathbb{P}}_k = k^2+4k+5 = \dim(\mathbb{P}_k^2 \oplus \mathbf{x}\tilde{\mathbb{P}}_k) + 2 = \dim\mathbf{V}_{\mathrm{AC}}^k.$$

When $k=0$, the number is $4\dim\mathbb{P}_k(e) = 4 = \dim(\mathbb{P}_0^2 \oplus \mathbf{x}\tilde{\mathbb{P}}_0) + 1 = \dim\mathbf{V}_{\mathrm{AC}}^0$.

It remains only to prove that the DOFs are unisolvent. We give a constructive proof. We construct a space of constant divergence vectors $\mathbb{E}_k \subset \mathbf{V}_{\mathrm{AC}}^{k,\mathrm{red}}$ that has a

basis for the edge DOFs (4.1), which we call a *constant divergence edge basis*. We also construct the space $\mathbb{B}_k$ of divergence-free vector functions in $\mathbf{V}_{\mathrm{AC}}^{k,\mathrm{red}}$ that have vanishing normal components, called *divergence-free bubbles*. The remaining vectors have nonconstant divergence (see Theorem 4.5), and the Helmholtz-like decomposition, Theorem 2.1, tells us that they lie in $\mathbf{x}\mathbb{P}_k$ for $\mathbf{V}_{\mathrm{AC}}^{k}$ and $\mathbf{x}\mathbb{P}_{k-1}$ for $\mathbf{V}_{\mathrm{AC}}^{k,\mathrm{red}}$.

4.1. Special linear polynomials. We now define special vector polynomials needed for construction of a constant divergence edge basis and divergence-free bubbles. Let E be a convex quadrilateral (assumed to be a closed set in the plane). We will orient it in the counterclockwise direction, as shown in Figure 1. The edge e_i has midpoint $\mathbf{x}_0^i$, outer unit normal ν_i, and unit tangent τ_i oriented by the right-hand rule from ν_i, for each $i = 1, 2, 3, 4$. The vertex "corner" $\mathbf{x}_c^i$ is labeled in the direction of τ_i from $\mathbf{x}_0^i$, so that $\mathbf{x}_c^i$ lies on e_i and e_{i+1}, where here and elsewhere the index is to be taken modulo 4.

The line joining midpoints $\mathbf{x}_0^2$ to $\mathbf{x}_0^4$ is called e_H, and it has unit "horizontal" normal ν_H pointing toward e_3 and unit tangent τ_H pointing toward e_4. The line e_V joins $\mathbf{x}_0^3$ to $\mathbf{x}_0^1$ and has "vertical" unit normal ν_V pointing toward e_4 and unit tangent τ_V pointing toward e_1. Let $\mathbf{x}_0 = \mathbf{x}_0^H = \mathbf{x}_0^V = e_H \cap e_V$ be the center of E, which is also the center of e_H and e_V.

We define local coordinates on E with respect to each edge e_i, $i = 1, 2, 3, 4$, as

$$\lambda_i(\mathbf{x}) = -(\mathbf{x} - \mathbf{x}_0^i) \cdot \nu_i, \tag{4.5}$$

$$\xi_i(\mathbf{x}) = (\mathbf{x} - \mathbf{x}_0^i) \cdot \tau_i. \tag{4.6}$$

It will be convenient to define the half-edge length as $L_i = \frac{1}{2}|e_i| = \frac{1}{2}\|\mathbf{x}_c^i - \mathbf{x}_c^{i-1}\|$. We also need two linear functions that are neutral with respect to opposite sides of the quadrilateral. Let

$$\lambda_H(\mathbf{x}) = -(\mathbf{x} - \mathbf{x}_0) \cdot \nu_H \quad \text{and} \quad \lambda_V(\mathbf{x}) = -(\mathbf{x} - \mathbf{x}_0) \cdot \nu_V. \tag{4.7}$$

Many results are easily shown about E, the local coordinates, and these two linear functions; we collect several facts that we will use.

LEMMA 4.1. *The following hold for any integer i and j (modulo 4):*

(a) $\tau_i = (-\nu_{i,2}, \nu_{i,1})$, $\tau_i \cdot \nu_j = -\tau_j \cdot \nu_i$, $\tau_i \cdot \nu_{i+1} > 0$, *and* $\tau_i \cdot \tau_j = \nu_i \cdot \nu_j$.
(b) $\lambda_i|_{e_i} = 0$ *and* $\lambda_i > 0$ *over* $E \setminus e_i$.
(c) $\xi_i(\mathbf{x}_c^{i-1}) = -L_i$, $\xi_i(\mathbf{x}_0^i) = 0$, *and* $\xi_i(\mathbf{x}_c^i) = L_i$.
(d) $\operatorname{curl} \lambda_i = \tau_i$ *and* $\operatorname{curl} \xi_i = \nu_i$.

Moreover, for $\alpha = H, V$ and any integer i (modulo 4), the following hold:

(e) $\tau_\alpha \cdot \nu_i = -\tau_i \cdot \nu_\alpha$, $\tau_H \cdot \nu_2 < 0$, $\tau_H \cdot \nu_4 > 0$, $\tau_V \cdot \nu_1 > 0$, *and* $\tau_V \cdot \nu_3 < 0$.
(f) *If e_1 and e_3 are parallel, then $\tau_H \cdot \nu_1 = \tau_H \cdot \nu_3 = 0$, and if e_2 and e_4 are parallel, then $\tau_V \cdot \nu_2 = \tau_V \cdot \nu_4 = 0$, but otherwise the expressions have indefinite sign.*
(g) $\lambda_\alpha|_{e_\alpha} = 0$.
(h) $\operatorname{curl} \lambda_\alpha = \tau_\alpha$.

We need to understand these six linear functions when restricted to the edges.

LEMMA 4.2. *For any integers i and j (modulo 4) and also for $i = H, V$,*

$$\lambda_i\big|_{e_j} = (\tau_i \cdot \nu_j)\, \xi_j\big|_{e_j} + (\mathbf{x}_0^i - \mathbf{x}_0^j) \cdot \nu_i. \tag{4.8}$$

Moreover, $(\mathbf{x}_0^i - \mathbf{x}_0^j) \cdot \nu_i \geq 0$ when i is an integer (modulo 4).

Proof. For any vector $\mathbf{v}$, by orthogonality,

$$\mathbf{v} = (\mathbf{v}\cdot\nu_i)\nu_i + (\mathbf{v}\cdot\tau_i)\tau_i, \quad i = 1,2,3,4,H,V.$$

Thus

$$\begin{aligned}\lambda_i\big|_{e_j} = -(\mathbf{x}-\mathbf{x}_0^i)\cdot\nu_i\big|_{e_j} &= -(\mathbf{x}-\mathbf{x}_0^j)\cdot\nu_i\big|_{e_j} - (\mathbf{x}_0^j-\mathbf{x}_0^i)\cdot\nu_i \\ &= -(\mathbf{x}-\mathbf{x}_0^j)\cdot[(\nu_i\cdot\nu_j)\nu_j + (\nu_i\cdot\tau_j)\tau_j]\big|_{e_j} - (\mathbf{x}_0^j-\mathbf{x}_0^i)\cdot\nu_i \\ &= -(\nu_i\cdot\tau_j)\xi_j\big|_{e_j} + (\mathbf{x}_0^i-\mathbf{x}_0^j)\cdot\nu_i,\end{aligned}$$

and Lemma 4.1(a) gives the main result. That $(\mathbf{x}_0^i-\mathbf{x}_0^j)\cdot\nu_i \geq 0$ when $i=1,2,3,4$ follows from the convexity of E. ∎

COROLLARY 4.3. *It holds for any integer i (modulo 4) that*

$$\lambda_i\big|_{e_{i-1}} = (\tau_i\cdot\nu_{i-1})\,(\xi_{i-1}-L_{i-1})\big|_{e_{i-1}} \iff \lambda_{i+1}\big|_{e_i} = (\tau_{i+1}\cdot\nu_i)\,(\xi_i-L_i)\big|_{e_i}, \tag{4.9}$$

$$\lambda_i\big|_{e_{i+1}} = (\tau_i\cdot\nu_{i+1})\,(\xi_{i+1}+L_{i+1})\big|_{e_{i+1}} \iff \lambda_{i-1}\big|_{e_i} = (\tau_{i-1}\cdot\nu_i)\,(\xi_i+L_i)\big|_{e_i}. \tag{4.10}$$

Moreover, $L_H = \frac{1}{2}(-\tau_V\cdot\nu_H)|e_V| = \frac{1}{2}(-\tau_V\cdot\nu_H)\|\mathbf{x}_0^1-\mathbf{x}_0^3\| > 0$ and

$$\lambda_H\big|_{e_1} = (\tau_H\cdot\nu_1)\,\xi_1\big|_{e_1} + L_H, \tag{4.11}$$

$$\lambda_H\big|_{e_2} = (\tau_H\cdot\nu_2)\,\xi_2\big|_{e_2}, \tag{4.12}$$

$$\lambda_H\big|_{e_3} = (\tau_H\cdot\nu_3)\,\xi_3\big|_{e_3} - L_H, \tag{4.13}$$

$$\lambda_H\big|_{e_4} = (\tau_H\cdot\nu_4)\,\xi_4\big|_{e_4}, \tag{4.14}$$

and $L_V = \frac{1}{2}(\tau_H\cdot\nu_V)|e_H| = \frac{1}{2}(\tau_H\cdot\nu_V)\|\mathbf{x}_0^4-\mathbf{x}_0^2\| > 0$ and

$$\lambda_V\big|_{e_1} = (\tau_V\cdot\nu_1)\,\xi_1\big|_{e_1}, \tag{4.15}$$

$$\lambda_V\big|_{e_2} = (\tau_V\cdot\nu_2)\,\xi_2\big|_{e_2} + L_V, \tag{4.16}$$

$$\lambda_V\big|_{e_3} = (\tau_V\cdot\nu_3)\,\xi_3\big|_{e_3}, \tag{4.17}$$

$$\lambda_V\big|_{e_4} = (\tau_V\cdot\nu_4)\,\xi_4\big|_{e_4} - L_V. \tag{4.18}$$

Proof. Results (4.9)–(4.18) follow directly from Lemma 4.2 once the constant terms in the expressions are evaluated. Each of these linear functions λ_i vanishes on its associated line e_i, $i = 1,2,3,4,H,V$ (Lemma 4.1(b), (g)). The results (4.9)–(4.10) hold by considering the corner points and invoking Lemma 4.1(c), and the results in (4.11)–(4.18) having a vanishing constant term hold trivially by considering the midpoints (where the local ξ-coordinate vanishes).

Now, the constant term in (4.11) is

$$\lambda_H(\mathbf{x}_0^1) = -(\mathbf{x}_0^1-\mathbf{x}_0)\cdot\nu_H = -\|\mathbf{x}_0^1-\mathbf{x}_0\|\tau_V\cdot\nu_H = -\tfrac{1}{2}\|\mathbf{x}_0^1-\mathbf{x}_0^3\|\tau_V\cdot\nu_H = L_H.$$

By symmetry, (4.13) has the opposite constant $-L_H$. Similarly, for (4.16),

$$\lambda_V(\mathbf{x}_0^2) = -(\mathbf{x}_0^2-\mathbf{x}_0)\cdot\nu_V = \|\mathbf{x}_0^2-\mathbf{x}_0\|\tau_H\cdot\nu_V = L_V,$$

and (4.18) follows by symmetry. ∎

4.2. Some special divergence-free vector polynomials. The vector polynomials that we will need for constructing a constant divergence edge basis are curls of products of the linear polynomials of the preceding section. The product rule implies that for any differentiable functions p and q, we have that

$$\operatorname{curl}(pq) = p \operatorname{curl} q + q \operatorname{curl} p. \tag{4.19}$$

Define the normal component or *flux* operator $\mathcal{F} : (C^0(E))^2 \to \prod_{i=1}^4 C^0(e_i)$ by

$$\mathcal{F}(\mathbf{v}) = \big(\mathbf{v}\cdot\nu_1|_{e_1}, \mathbf{v}\cdot\nu_2|_{e_2}, \mathbf{v}\cdot\nu_3|_{e_3}, \mathbf{v}\cdot\nu_4|_{e_4}\big). \tag{4.20}$$

It is instructive to note that for $i = 1, 2$ (modulo 4),

$$\operatorname{curl}(\lambda_i\lambda_{i+2}) = \lambda_i\tau_{i+2} + \lambda_{i+2}\tau_i \tag{4.21}$$

by Lemma 4.1(d). Corollary 4.3 shows that

$$\mathcal{F}\big(\operatorname{curl}(\lambda_1\lambda_3)\big) = \big(0, 2(\tau_1\cdot\nu_2)(\tau_3\cdot\nu_2)\,\xi_2, 0, 2(\tau_1\cdot\nu_4)(\tau_3\cdot\nu_4)\,\xi_4\big), \tag{4.22}$$

$$\mathcal{F}\big(\operatorname{curl}(\lambda_2\lambda_4)\big) = \big(2(\tau_2\cdot\nu_1)(\tau_4\cdot\nu_1)\,\xi_1, 0, 2(\tau_2\cdot\nu_3)(\tau_4\cdot\nu_3)\,\xi_3, 0\big), \tag{4.23}$$

and so these vectors have normal components vanishing on opposite sides of the quadrilateral. For any differentiable function λ,

$$\operatorname{curl}(\lambda_i\lambda_{i+2}\,\lambda) = \operatorname{curl}(\lambda_i\lambda_{i+2})\,\lambda + \lambda_i\lambda_{i+2}\operatorname{curl}\lambda$$

also has no normal component flux on sides e_i and e_{i+2}.

For $n = 0, 1, 2, \ldots$, we define vector polynomials analogous on the square $\hat{E} = [-1, 1]^2$ to curls of $(-\hat{x})^n(1-\hat{x}^2)$ and $(-\hat{x})^n(1-\hat{x}^2)(-\hat{y})$ as

$$\mathbf{v}_H^{n+1} = \operatorname{curl}(\lambda_1\lambda_3\lambda_H^n) \in \mathbb{P}^2_{n+1}, \tag{4.24}$$

$$\mathbf{v}_{HV}^{n+2} = \operatorname{curl}(\lambda_1\lambda_3\lambda_H^n\lambda_V) \in \mathbb{P}^2_{n+2}. \tag{4.25}$$

Similarly, analogues to curls of $(-\hat{y})^n(1-\hat{y}^2)$ and $(-\hat{x})(-\hat{y})^n(1-\hat{y}^2)$ are

$$\mathbf{v}_V^{n+1} = \operatorname{curl}(\lambda_2\lambda_4\lambda_V^n) \in \mathbb{P}^2_{n+1}, \tag{4.26}$$

$$\mathbf{v}_{VH}^{n+2} = \operatorname{curl}(\lambda_2\lambda_4\lambda_V^n\lambda_H) \in \mathbb{P}^2_{n+2}. \tag{4.27}$$

These vector polynomials have relatively simple normal components on all four edges of E, as stated carefully in the following theorem.

We describe briefly what is important for each pair in general but imprecise terms. The pair $\mathbf{v}_H^{n+1}$ and $\mathbf{v}_{HV}^{n+2}$ have no normal flux on sides e_1 and e_3. On the other two sides, they have polynomial normal flux of order $n+1$, but in such a way that the sign of $\mathcal{F}_2(\mathbf{v}_H^{n+1})\mathcal{F}_4(\mathbf{v}_H^{n+1})$ differs from $\mathcal{F}_2(\mathbf{v}_{HV}^{n+2})\mathcal{F}_4(\mathbf{v}_{HV}^{n+2})$, and therefore these two vectors will form a basis for polynomials of degree $n+1$ on edges e_2 and e_4. The only problem is that to achieve the change in sign, $\mathbf{v}_{HV}^{n+2}$ incorporated λ_V, and so we obtain also polynomials of degree $n+2$ in the fluxes. We will resolve the problem in the next section. The pair $\mathbf{v}_V^{n+1}$ and $\mathbf{v}_{VH}^{n+2}$ has similar properties for the opposite edges.

THEOREM 4.4. *Fix integer $n \geq 0$ and for each $i = 1, 2, 3, 4$, let*

$$p_i^{n+1}(\xi) = \big[(n+2)\xi^2 - nL_i^2\big]\,\xi^{n-1} \in \mathbb{P}_{n+1}. \tag{4.28}$$

For each $i = 2, 4$, let

$$b_{n+1} = (\tau_1\cdot\nu_2)(-\tau_3\cdot\nu_2)(-\tau_H\cdot\nu_2)^n > 0, \tag{4.29}$$

$$d_{n+1} = (-\tau_1\cdot\nu_4)(\tau_3\cdot\nu_4)(\tau_H\cdot\nu_4)^n > 0, \tag{4.30}$$

and then

$$\mathcal{F}(\mathbf{v}_H^{n+1}) = \big(0, (-1)^{n+1} b_{n+1}\, p_2^{n+1}(\xi_2), 0, -d_{n+1}\, p_4^{n+1}(\xi_4)\big), \tag{4.31}$$

$$\mathcal{F}(\mathbf{v}_{HV}^{n+2}) = \bigg(0, (-1)^{n+1} \frac{\tau_V \cdot \nu_2}{\tau_H \cdot \nu_2} b_{n+2}\, p_2^{n+2}(\xi_2) + (-1)^{n+1} L_V\, b_{n+1}\, p_2^{n+1}(\xi_2), \\ 0, -\frac{\tau_V \cdot \nu_4}{\tau_H \cdot \nu_4} d_{n+2}\, p_4^{n+2}(\xi_4) + L_V\, d_{n+1}\, p_4^{n+1}(\xi_4)\bigg), \tag{4.32}$$

where $\tau_V \cdot \nu_2 = \tau_V \cdot \nu_4 = 0$ *if* e_2 *and* e_4 *are parallel. For each* $i = 1, 3$*, let*

$$a_{n+1} = (-\tau_2 \cdot \nu_1)(\tau_4 \cdot \nu_1)(\tau_V \cdot \nu_1)^n > 0, \tag{4.33}$$

$$c_{n+1} = (\tau_2 \cdot \nu_3)(-\tau_4 \cdot \nu_3)(-\tau_V \cdot \nu_3)^n > 0, \tag{4.34}$$

and then

$$\mathcal{F}(\mathbf{v}_V^{n+1}) = \big(- a_{n+1}\, p_1^{n+1}(\xi_1), 0, (-1)^{n+1} c_{n+1}\, p_3^{n+1}(\xi_3), 0\big), \tag{4.35}$$

$$\mathcal{F}(\mathbf{v}_{VH}^{n+2}) = \bigg(- \frac{\tau_H \cdot \nu_1}{\tau_V \cdot \nu_1} a_{n+2}\, p_1^{n+2}(\xi_1) - L_H\, a_{n+1}\, p_1^{n+1}(\xi_1), 0, \\ (-1)^{n+1} \frac{\tau_H \cdot \nu_3}{\tau_V \cdot \nu_3} c_{n+2}\, p_3^{n+2}(\xi_3) - (-1)^{n+1} L_H\, c_{n+1}\, p_3^{n+1}(\xi_3), 0\bigg), \tag{4.36}$$

where $\tau_H \cdot \nu_1 = \tau_H \cdot \nu_3 = 0$ *if* e_1 *and* e_3 *are parallel. Moreover,*

$$\begin{aligned} &\mathcal{F}(\operatorname{curl}(\lambda_H \lambda_V)) \\ &\quad = \big((\tau_V \cdot \nu_1)[(\tau_H \cdot \nu_1)\, p_1^1(\xi_1) + L_H], (-\tau_H \cdot \nu_2)[-(\tau_V \cdot \nu_2)\, p_2^1(\xi_2) - L_V], \\ &\qquad (-\tau_V \cdot \nu_3)[-(\tau_H \cdot \nu_3)\, p_3^1(\xi_3) + L_H], (\tau_H \cdot \nu_4)[(\tau_V \cdot \nu_4)\, p_4^1(\xi_4) - L_V]\big), \end{aligned} \tag{4.37}$$

wherein the coefficients of L_H *and* L_V *are strictly positive and negative, respectively.*

Proof. The signs of the dot products follow from Lemma 4.1(a), (e), (f). We saw already the two vanishing normal components in (4.31)–(4.32) on e_1 and e_3. We prove the rest of (4.31) by induction, which starts for $n = 0$ by (4.22). So assume that the result holds for n and consider side e_i, $i = 2, 4$. By Lemma 4.1(d), (h) and Corollary 4.3, we have on e_2 that

$$\begin{aligned} \mathcal{F}_2(\mathbf{v}_H^{n+2}) &= \operatorname{curl}\big((\lambda_1 \lambda_3 \lambda_H^n)\lambda_H\big) \cdot \nu_2 \\ &= \mathbf{v}_H^{n+1} \cdot \nu_2\, \lambda_H + \lambda_1 \lambda_3 \lambda_H^n\, \tau_H \cdot \nu_2 \\ &= (-1)^{n+1} b_{n+1}\, p_2^{n+1}(\xi_2)\, (\tau_H \cdot \nu_2)\, \xi_2 + (\tau_1 \cdot \nu_2)(\tau_3 \cdot \nu_2)\, (\xi_2^2 - L_2^2)\, (\tau_H \cdot \nu_2)^{n+1} \xi_2^n \\ &= (-1)^{n+1} b_{n+1}\, (\tau_H \cdot \nu_2)\big[p_2^{n+1}(\xi_2)\, \xi_2 + (\xi_2^2 - L_2^2)\, \xi_2^n\big] \\ &= (-1)^{n+2} b_{n+2}\, p_2^{n+2}(\xi_2), \end{aligned}$$

and similarly on e_4, so the induction is shown.

For (4.32), using (4.31), Lemma 4.1(d), (h), Corollary 4.3, and the above calculation, we compute on e_2 (and similarly on e_4) that

$$\begin{aligned}
\mathcal{F}_2(\mathbf{v}_{HV}^{n+2}) &= \operatorname{curl}\big((\lambda_1\lambda_3\lambda_H^n)\lambda_V\big)\cdot\nu_2 \\
&= \mathbf{v}_H^{n+1}\cdot\nu_2\,\lambda_V + \lambda_1\lambda_3\lambda_H^n\,\tau_V\cdot\nu_2 \\
&= (-1)^{n+1}b_{n+1}\,p_2^{n+1}(\xi_2)[(\tau_V\cdot\nu_2)\,\xi_2 + L_V] \\
&\quad + (\tau_1\cdot\nu_2)(\tau_3\cdot\nu_2)(\xi_2^2 - L_2^2)(\tau_H\cdot\nu_2)^n\xi_2^n(\tau_V\cdot\nu_2) \\
&= (\tau_V\cdot\nu_2)\big[(-1)^{n+1}b_{n+1}\,p_2^{n+1}(\xi_2)\,\xi_2 + (\tau_1\cdot\nu_2)(\tau_3\cdot\nu_2)(\xi_2^2 - L_2^2)(\tau_H\cdot\nu_2)^n\xi_2^n\big] \\
&\quad + (-1)^{n+1}b_{n+1}\,p_2^{n+1}(\xi_2)\,L_V \\
&= (-1)^{n+2}\frac{\tau_V\cdot\nu_2}{\tau_H\cdot\nu_2}b_{n+2}\,p_2^{n+2}(\xi_2) + (-1)^{n+1}L_V b_{n+1}\,p_2^{n+1}(\xi_2).
\end{aligned}$$

The two results (4.35)–(4.36) can be verified similarly, as can the final result, for which, e.g.,

$$\begin{aligned}
\mathcal{F}_1\big(\operatorname{curl}(\lambda_H\lambda_V)\big) &= (\tau_H\cdot\nu_1)\,\lambda_V + (\tau_V\cdot\nu_1)\lambda_H \\
&= (\tau_H\cdot\nu_1)(\tau_V\cdot\nu_1)\,\xi_1 + (\tau_V\cdot\nu_1)[(\tau_H\cdot\nu_1)\,\xi_1 + L_H] \\
&= (\tau_H\cdot\nu_1)(\tau_V\cdot\nu_1)\,p_1^1(\xi_1) + (\tau_V\cdot\nu_1)\,L_H,
\end{aligned}$$

and similarly for the other edges. ∎

4.3. Construction of a constant divergence edge basis. We are now ready to construct the space of constant divergence edge basis vectors for $\mathbb{E}_k$, using the choice (3.15) for $\mathbb{S}_k$. We begin with a remark about the Piola mapping $\mathcal{P}$. We know that the Piola transform preserves edge normal components in the sense of (3.6). Consider a reference polynomial $\hat{\mathbf{v}}(\hat{x},\hat{y})$ defined on $\hat{E} = [-1,1]^2$. On side $\hat{e}_i$, the normal component is the polynomial $\hat{\mathbf{v}}\cdot\hat{\nu}_i(\hat{z})$, where $\hat{z}$ is either $\hat{x}$ ($i = 1,3$) or $\hat{y}$ ($i = 2,4$). Notice that these local coordinates have the wrong sign on edges e_1 and e_4 compared to the orientation of our local coordinates ξ_i on the counterclockwise oriented quadrilateral E. Let $s_1 = s_4 = -1$ and $s_2 = s_3 = 1$, so that the change of variables to E is $\xi_i = s_i L_i\hat{z}$. Moreover, there is a Jacobian factor in the transformation of size L_i, and so $\hat{\mathbf{v}}\cdot\hat{\nu}(\hat{z})$ on e_i transforms to $\mathbf{v}\cdot\nu(\xi_i) = \hat{\mathbf{v}}\cdot\hat{\nu}(s_i\xi_i/L_i)/L_i$; that is, a monomial transforms according to the rule

$$\hat{z}^n \quad \overset{\mathcal{P}_E}{\longmapsto} \quad \frac{(s_i\xi_i)^n}{L_i^{n+1}}. \tag{4.38}$$

We first construct the constant divergence edge basis for $\mathbb{E}_0$, which is the entire lowest order full $H(\operatorname{div})$-approximation space $\mathbf{V}_{\mathrm{AC}}^0 = \mathbb{P}_0^2 \oplus \mathbf{x}\mathbb{P}_0 \oplus \mathbb{S}_0$. In this case, $\mathbb{S}_0 = \operatorname{span}\{\mathcal{P}_E\operatorname{curl}(\hat{x}\hat{y})\}$ has only dimension one and $\mathbb{E}_0$ has dimension four. Let

$$\mathbf{v}_i^0 = \mathbf{x} - \mathbf{x}_c^i \in \mathbb{P}_0^2 \oplus \mathbf{x}\mathbb{P}_0 \subset \mathbf{V}_{\mathrm{AC}}^0, \tag{4.39}$$

$$\sigma^0 = \mathcal{P}_E\operatorname{curl}(\hat{x}\hat{y}). \tag{4.40}$$

The normal components of $\hat{\sigma}^0 = (\hat{x},-\hat{y})$ are

$$\hat{\mathcal{F}}(\hat{\sigma}^0) = (1,-1,1,-1).$$

The normal components of, say, $\mathbf{v}_1^0$ are constant and vanish on e_1 and e_2 (since $\mathbf{x}_c^1 \in e_1\cap e_2$), but on the other edges they are

$$\mathbf{v}_1^0\cdot\nu_3|_{e_3}=\mathbf{v}_1^0\cdot\nu_3(\mathbf{x}_c^2)=(\mathbf{x}_c^2-\mathbf{x}_c^1)\cdot\nu_3=2L_2\tau_2\cdot\nu_3,$$
$$\mathbf{v}_1^0\cdot\nu_4|_{e_4}=\mathbf{v}_1^0\cdot\nu_4(\mathbf{x}_c^4)=(\mathbf{x}_c^4-\mathbf{x}_c^1)\cdot\nu_4=-2L_1\tau_1\cdot\nu_4=2L_1\tau_4\cdot\nu_1.$$

Similarly we compute the other fluxes and arrive at

$$\text{(4.41)}\qquad\begin{cases}\mathcal{F}(\mathbf{v}_2^0)=(2L_2\tau_1\cdot\nu_2,\ 0,\ 0,\ 2L_3\tau_3\cdot\nu_4),\\ \mathcal{F}(\mathbf{v}_4^0)=(0,\ 2L_1\tau_1\cdot\nu_2,\ 2L_4\tau_3\cdot\nu_4,\ 0\ ),\\ \mathcal{F}(\mathbf{v}_1^0)=(0,\ 0,\ 2L_2\tau_2\cdot\nu_3,\ 2L_1\tau_4\cdot\nu_1),\\ \mathcal{F}(\sigma^0)=(L_1^{-1},\ -L_2^{-1},\ L_3^{-1},\ -L_4^{-1}\ ),\end{cases}$$

wherein each dot product is positive by Lemma 4.1(a). Thought of as a matrix, the determinant is negative, and so linear combinations of $\mathbf{v}_1^0$, $\mathbf{v}_2^0$, $\mathbf{v}_4^0$, and σ^0 give a constant divergence edge basis, i.e., $\{\tilde{\mathbf{v}}_1^0,\tilde{\mathbf{v}}_2^0,\tilde{\mathbf{v}}_3^0,\tilde{\mathbf{v}}_4^0\ :\ \tilde{\mathbf{v}}_i^0\cdot\nu_j|_{e_j}=\delta_{ij}\}$, and the span forms $\mathbb{E}_0=\mathbf{V}_{\mathrm{AC}}^0$.

Now assume that $k\ge1$. We construct a basis for $\mathbb{E}_k$ within $x\mathbb{P}_0\oplus\operatorname{curl}\mathbb{P}_{k+1}\oplus\mathbb{S}_k$, so the divergence of each vector is constant. In fact, we set

$$\text{(4.42)}\qquad\begin{aligned}\mathbb{E}_k=\big(\operatorname{span}\{\mathbf{v}_H^k,\mathbf{v}_V^k\}\oplus\mathbb{S}_k\big)\oplus\operatorname{span}\{\mathbf{v}_H^{k-1},\mathbf{v}_V^{k-1},\mathbf{v}_{HV}^k,\mathbf{v}_{VH}^k\}\\ \oplus\cdots\oplus\operatorname{span}\{\mathbf{v}_H^1,\mathbf{v}_V^1,\mathbf{v}_{HV}^2,\mathbf{v}_{VH}^2\}\oplus\operatorname{span}\{\mathbf{v}_1^0,\mathbf{v}_2^0,\mathbf{v}_4^0,\operatorname{curl}(\lambda_H\lambda_V)\},\end{aligned}$$

which has the required dimension $4(k+1)$. We must prove that this space contains a constant divergence edge basis, and we will do so by noting that the polynomials from Theorem 4.4, $p_i^n(\xi_i)$, $n=0,1,\dots,k$, with $p_i^0=1$, form a basis for $\mathbb{P}_k(e_i)$.

The edge fluxes of $\hat\sigma_1=\operatorname{curl}(\hat x^{k-1}(1-\hat x^2)\hat y)$ and $\hat\sigma_2=\operatorname{curl}(\hat x\hat y^{k-1}(1-\hat y^2))$ are

$$\hat{\mathcal{F}}(\hat\sigma_1^k)=\big(0,-[(k+1)\hat x^2-(k-1)]\hat x^{k-2},0,-[(k+1)\hat x^2-(k-1)]\hat x^{k-2}\big),$$
$$\hat{\mathcal{F}}(\hat\sigma_2^k)=\big([(k+1)\hat y^2-(k-1)]\hat y^{k-2},0,[(k+1)\hat y^2-(k-1)]\hat y^{k-2},0\big).$$

Under the Piola transformation, (4.38) tells us that

$$[(k+1)\hat z^2-(k-1)]\hat z^{k-2}\xrightarrow{\mathcal{P}_E}s_i^kL_i^{-k-1}[(k+1)\xi_i^2-(k-1)L_i^2]\xi_i^{k-2}=s_i^kL_i^{-k-1}p_i^k(\xi_i),$$

and so

$$\text{(4.43)}\qquad\mathcal{F}(\sigma_1^k)=\big(0,-L_2^{-k-1}p_2^k(\xi_2),0,-(-1)^kL_4^{-k-1}p_4^k(\xi_4)\big),$$
$$\text{(4.44)}\qquad\mathcal{F}(\sigma_2^k)=\big((-1)^kL_1^{-k-1}p_1^k(\xi_1),0,L_3^{-k-1}p_3^k(\xi_3),0\big).$$

Comparing the fluxes for σ_1 with those of $\mathbf{v}_H^k$ in (4.31), we see linear independence (the signs of the terms do *not* match). Similarly, σ_2 and $\mathbf{v}_V^k$ have linearly independent fluxes. Thus we can construct $\tilde{\mathbf{v}}_i^k$ having only the nonvanishing flux $p_i^k(\xi_i)$ on edge e_i, $i=1,2,3,4$, which gives a basis for the highest order terms.

For the next order terms, we use $\tilde{\mathbf{v}}_2^k$ and $\tilde{\mathbf{v}}_4^k$ to remove the higher order terms from $\mathbf{v}_{HV}^k$ (if necessary), and then comparing the remaining fluxes to those of $\mathbf{v}_H^{k-1}$ shows that they are linearly independent (again the signs of the terms do *not* match). Similarly we treat $\mathbf{v}_{VH}^k$ and $\mathbf{v}_V^{k-1}$. We can then construct $\tilde{\mathbf{v}}_i^{k-1}$ having only the nonvanishing flux $p_i^{k-1}(\xi_i)$ on edge e_i, $i=1,2,3,4$, which gives a basis for the terms of order $k-1$.

We can continue this process to form $\tilde{\mathbf{v}}_i^j$ having only the nonvanishing flux $p_i^j(\xi_i)$ on edge e_i, $i = 1, 2, 3, 4$, for $j = 1, 2, \ldots, k$. At the lowest level, we need to argue as in the case for $k = 0$, i.e., (4.41). We replace σ_0 by $\operatorname{curl}(\lambda_H \lambda_V)$, for which the edge flux is given in (4.37) and, with $\tilde{\mathbf{v}}_i^1$, $i = 1, 2, 3, 4$, allows a similar construction of the remaining functions $\tilde{\mathbf{v}}_i^0$, $i = 1, 2, 3, 4$. The existence of a constant divergence edge basis is thereby established.

4.4. Construction of divergence-free bubbles. Set $\mathbb{B}_0 = \mathbb{B}_1 = \mathbb{B}_2 = \{0\}$, and for $k \geq 3$, define the space of vector polynomials

$$\mathbb{B}_k = \operatorname{curl}(\lambda_1 \lambda_2 \lambda_3 \lambda_4 \mathbb{P}_{k-3}) \subset \mathbb{P}_k^2. \tag{4.45}$$

Each is a divergence-free bubble, since the normal components vanish on ∂E. In fact, we claim that these are the only such bubbles, which is implied by the following result.

THEOREM 4.5. *For index k,*

$$\mathbf{V}_{\mathrm{AC}}^{k,\mathrm{red}}(E) = \mathbb{P}_k^2 \oplus \mathbb{S}_k \qquad = \mathbf{x}\mathbb{P}_{k-1}^* \oplus \mathbb{E}_k \oplus \mathbb{B}_k, \quad k \geq 1, \tag{4.46}$$

$$\mathbf{V}_{\mathrm{AC}}^{k}(E) = \mathbb{P}_k^2 \oplus \mathbf{x}\tilde{\mathbb{P}}_k \oplus \mathbb{S}_k = \mathbf{x}\mathbb{P}_k^* \oplus \mathbb{E}_k \oplus \mathbb{B}_k, \qquad k \geq 0, \tag{4.47}$$

where $\mathbb{P}_{k-1}^* = \bigoplus_{n=1}^{k-1} \tilde{\mathbb{P}}_n$, which is $\mathbb{P}_{k-1}$ without the constants $\tilde{\mathbb{P}}_0 = \mathbb{P}_0$.

Proof. The case $k = 0$ was established in section 4.3, so it is sufficient to prove (4.46). That any pair of spaces intersect at $\{0\}$ is easily established as follows. First, if $\mathbf{v} \in \mathbf{x}\mathbb{P}_{k-1}^* \cap (\mathbb{E}_k + \mathbb{B}_k)$, then $\nabla \cdot \mathbf{v} \in \mathbb{P}_{k-1}^* \cap \mathbb{P}_0 = \{0\}$ and so $\mathbf{v} = 0$ by Theorem 2.1 (the divergence is a one-to-one map on $\mathbf{x}\tilde{\mathbb{P}}_j$). Second, if $\mathbf{v} \in \mathbb{E}_k \cap \mathbb{B}_k$, then the edge normal components vanish and, again, $\mathbf{v} = 0$.

Since $\dim \mathbf{V}_{\mathrm{AC}}^{k,\mathrm{red}}(E) = (k+2)(k+1)+2$ is the sum of $\dim \mathbf{x}\mathbb{P}_{k-1}^* = \frac{1}{2}(k+1)k-1$, $\dim \mathbb{E}_k = 4(k+1)$, and $\dim \mathbb{B}_k = \frac{1}{2}(k-1)(k-2)$, the result is established. ∎

This result and Theorem 2.1 show that our new spaces are of minimal dimension subject to the locality and polynomial approximation properties. The space $\mathbb{E}_k$ is needed for locality, and the space $\mathbf{x}\mathbb{P}_{k-1}^*$ or $\mathbf{x}\mathbb{P}_k^*$ is needed for divergence approximation. These two spaces are linearly independent. The remaining part, $\mathbb{B}_k$, contributes nothing to locality and divergence approximation, but it is needed for local polynomial approximation in $(L^2)^2$.

4.5. Unisolvence of the DOFs. Unisolvence of the DOFs (4.1)–(4.3) for $\mathbf{V}_{\mathrm{AC}}^{k,\mathrm{red}}$ and DOFs (4.1)–(4.4) for $\mathbf{V}_{\mathrm{AC}}^{k}$ follow from Theorem 4.5. Let $\ell = k-1$ for $\mathbf{V}_{\mathrm{AC}}^{k,\mathrm{red}}$ and $\ell = k$ for $\mathbf{V}_{\mathrm{AC}}^{k}$. Suppose that $\mathbf{v}_h \in \mathbf{V}_{\mathrm{AC}}^{k,\mathrm{red}}$ or $\mathbf{v}_h \in \mathbf{V}_{\mathrm{AC}}^{k}$ has vanishing DOFs. We decompose

$$\mathbf{v}_h = \mathbf{v}_{\mathrm{div}} + \mathbf{v}_{\mathbb{E}} + \mathbf{v}_{\mathbb{B}} \in \mathbf{x}\mathbb{P}_\ell^* \oplus \mathbb{E}_k \oplus \mathbb{B}_k \quad \text{(respectively)}.$$

We first note that vanishing DOFs (4.1) and (4.2) (and (4.4)) imply that, for any $w \in \tilde{\mathbb{P}}_\ell$,

$$0 = (\mathbf{v}_h, \nabla w)_E = -(\nabla \cdot \mathbf{v}_h, w)_E, \tag{4.48}$$

and thus $\nabla \cdot \mathbf{v}_h = 0$. We conclude that $\mathbf{v}_{\mathrm{div}} = 0$. DOFs (4.1) now imply that $\mathbf{v}_{\mathbb{E}} = 0$, and finally (4.3) shows that $\mathbf{v}_{\mathbb{B}} = 0$, and thus $\mathbf{v}_h = 0$ and the unisolvence, and therefore the existence of the π operator and global consistency, is verified.

5. Issues of implementation. In the hybrid form of the mixed method [4], the Lagrange multiplier space on the edge e is simply $\mathbb{P}_k(e)$, and implementation is clear up to evaluation of the integrals over the elements. If the hybrid form is not used, one needs $H(\mathrm{div})$-conforming finite element shape functions to from a local basis.

5.1. A practical basis of edge and bubble vector shape functions. To create $H(\mathrm{div})$-conforming finite element shape functions, we need to match edge DOFs between elements. All other shape functions are local to the element.

The basis constructed in section 4.3 for $\mathbb{E}_k$ has the advantage that it has constant divergence. However, it is not necessarily the most convenient basis to construct and implement. A simpler edge basis can be constructed using vector polynomials in the full $H(\mathrm{div})$-approximating space, at least when $k \geq 1$. The cases $k = 0$ for full and $k = 1$ for reduced approximation are special, and a general basis for these cases can be constructed much like in (4.41) by taking linear combinations of the simple vector polynomials constructed in the previous section.

We proceed assuming that we are implementing the full $H(\mathrm{div})$-approximating space $\mathbf{V}^k_{\mathrm{AC}}$, $k \geq 1$, and we work locally on an element $E \in \mathcal{T}_h$. Because $\mathbb{P}_1 \oplus \mathbf{x}\tilde{\mathbb{P}}_1$ is in the space, we have, e.g., on side e_1 the two vector polynomials

$$\mathbf{v}_1^- = \frac{(\mathbf{x} - \mathbf{x}_c^3)\lambda_2}{2L_1L_4(\tau_2 \cdot \nu_1)(\tau_4 \cdot \nu_1)} \quad \text{and} \quad \mathbf{v}_1^+ = \frac{-(\mathbf{x} - \mathbf{x}_c^2)\lambda_4}{2L_1L_2(\tau_2 \cdot \nu_1)(\tau_4 \cdot \nu_1)}, \tag{5.1}$$

for which the normal components on the other three sides vanish. On e_1, Corollary 4.3 shows that

$$(\mathbf{x} - \mathbf{x}_c^3) \cdot \nu_1 \, \lambda_2|_{e_1} = (\mathbf{x}_c^4 - \mathbf{x}_c^3) \cdot \nu_1 \, (\tau_2 \cdot \nu_1)(\xi_1 - L_1) = 2L_4(\tau_4 \cdot \nu_1)(\tau_2 \cdot \nu_1)(\xi_1 - L_1),$$

and so $\mathbf{v}_1^- \cdot \nu_1|_{e_1} = (\xi_1 - L_1)/L_1$. Similarly, $\mathbf{v}_1^+ \cdot \nu_1|_{e_1} = (\xi_1 + L_1)/L_1$, and these two form a basis for $\mathbb{P}_1(e_1)$. A basis, i.e., the shape functions, for $\mathbb{P}_k(e_1)$ is then given by

$$\mathbf{v}_1^0 = \tfrac{1}{2}(\mathbf{v}_1^+ - \mathbf{v}_1^-) \qquad \in \mathbb{P}_1 \oplus \mathbf{x}\tilde{\mathbb{P}}_1, \tag{5.2}$$

$$\mathbf{v}_1^n = \tfrac{1}{2}(\mathbf{v}_1^+ + \mathbf{v}_1^-)(\xi_1/L_1)^{n-1} \in \mathbb{P}_n \oplus \mathbf{x}\tilde{\mathbb{P}}_n, \quad n = 1, 2, \ldots, k. \tag{5.3}$$

Note that when $e_1 = E^- \cap E^+$ is the edge between elements E^- and E^+, these vector functions constructed on each element will match on e_1. In a similar way we construct $\mathbf{v}_i^n$ for each edge e_i, $i = 1, 2, 3, 4$ and $n = 1, 2, \ldots, k$. These shape functions are easily constructed, and so they form a better basis to use in practice. The span is the edge space

$$\breve{\mathbb{E}}_k = \mathrm{span}\{\mathbf{v}_i^n \,:\, i = 1, 2, 3, 4 \text{ and } n = 0, 1, \ldots, k\}. \tag{5.4}$$

The rest of the finite element space $\mathbf{V}^k_{\mathrm{AC}}(E)$ consists of the supplemental space $\mathbb{S}_k$ and the space of (not necessarily divergence-free) bubble functions $\breve{\mathbb{B}}_k$, i.e., vector polynomials with vanishing normal components on the edges of the elements. Its local dimension is

$$\dim \breve{\mathbb{B}}_k = \dim \mathbb{P}_k^2 \oplus \mathbf{x}\tilde{\mathbb{P}}_k - \dim \breve{\mathbb{E}}_k = (k+3)(k+1) - 4(k+1) = k^2 - 1,$$

and bubble functions exist only when $k \geq 2$. Within $\mathbb{P}_2 \oplus \mathbf{x}\tilde{\mathbb{P}}_2$ we construct three linearly independent bubbles using the points $\mathbf{x}_c^{1,3} = e_1 \cap e_3$ and $\mathbf{x}_c^{2,4} = e_2 \cap e_4$ (wherein we extend each edge to a line), which exist provided the opposite sides are not parallel. The bubbles are

$$\mathbf{v}_{B,1} = \begin{cases} (\mathbf{x} - \mathbf{x}_c^{1,3})\lambda_2\lambda_4 & \text{if} \quad e_1 \not\parallel e_3 \text{ (i.e., } \tau_1 \neq -\tau_3), \\ \tau_1\lambda_2\lambda_4 & \text{if} \quad e_1 \parallel e_3 \text{ (i.e., } \tau_1 = -\tau_3), \end{cases} \tag{5.5}$$

$$\mathbf{v}_{B,2} = \begin{cases} (\mathbf{x} - \mathbf{x}_c^{2,4})\lambda_1\lambda_3 & \text{if} \quad e_2 \not\parallel e_4 \text{ (i.e., } \tau_2 \neq -\tau_4), \\ \tau_2\lambda_1\lambda_3 & \text{if} \quad e_2 \parallel e_4 \text{ (i.e., } \tau_2 = -\tau_4), \end{cases} \tag{5.6}$$

$$\mathbf{v}_{B,3} = (\mathbf{x} - \mathbf{x}_c^1)\lambda_3\lambda_4. \tag{5.7}$$

The space $\breve{\mathbb{B}}_k$ is then

$$\breve{\mathbb{B}}_k = \mathbf{v}_{B,1}\mathbb{P}_{k-2} \oplus \mathbf{v}_{B,2}\mathbb{P}_{k-2} \oplus \mathbf{v}_{B,3}\tilde{\mathbb{P}}_{k-2} \subset \mathbb{P}_k^2 \oplus \mathbf{x}\tilde{\mathbb{P}}_k, \tag{5.8}$$

which indeed has dimension $\frac{1}{2}k(k-1) + \frac{1}{2}k(k-1) + (k-1) = k^2 - 1$, provided the three spaces are linearly independent.

To prove the linear independence in (5.8), suppose without loss of generality that we translate so that $\mathbf{x}_c^1 = 0$. Then we ask if there are nonvanishing polynomials $p, q \in \mathbb{P}_{k-2}$ and $r \in \tilde{\mathbb{P}}_{k-2}$ such that $\mathbf{v}_{B,1}\, p + \mathbf{v}_{B,2}\, q = \mathbf{v}_{B,3}\, r$. The harder case is when the edges are not parallel, so let us proceed with

$$(\mathbf{x} - \mathbf{x}_c^{1,3})\lambda_2\lambda_4\, p + (\mathbf{x} - \mathbf{x}_c^{2,4})\lambda_1\lambda_3\, q = \mathbf{x}\lambda_3\lambda_4\, r.$$

By inspection, there are polynomials $\check{p}, \check{q} \in \mathbb{P}_{k-3}$ such that $p = \lambda_3\check{p}$ and $q = \lambda_4\check{q}$, so the case $k = 2$ is shown and we reduce the condition to

$$(\mathbf{x} - \mathbf{x}_c^{1,3})\lambda_2\, \check{p} + (\mathbf{x} - \mathbf{x}_c^{2,4})\lambda_1\, \check{q} = \mathbf{x}\, r \quad \text{for } k \geq 3.$$

Note that $\mathbf{x}_c^1 = 0$ implies that $\lambda_1 = \mathbf{x} \cdot \nu_1$ and $\lambda_2 = \mathbf{x} \cdot \nu_2$. Moreover, in a similar way $(\mathbf{x} - \mathbf{x}_c^{1,3}) \cdot \nu_1 = \mathbf{x} \cdot \nu_1$ and $(\mathbf{x} - \mathbf{x}_c^{2,4}) \cdot \nu_2 = \mathbf{x} \cdot \nu_2$. Taking the dot product with ν_1 and ν_2, we see that

$$\begin{aligned} \mathbf{x} \cdot \nu_1\, \mathbf{x} \cdot \nu_2\, \check{p} + (\mathbf{x} - \mathbf{x}_c^{2,4}) \cdot \nu_1\, \mathbf{x} \cdot \nu_1\, \check{q} &= \mathbf{x} \cdot \nu_1\, r, \\ (\mathbf{x} - \mathbf{x}_c^{1,3}) \cdot \nu_2\, \mathbf{x} \cdot \nu_2\, \check{p} + \mathbf{x} \cdot \nu_2\, \mathbf{x} \cdot \nu_1\, \check{q} &= \mathbf{x} \cdot \nu_2\, r, \end{aligned}$$

and so

$$-\mathbf{x}_c^{2,4} \cdot \nu_1\, \check{q} = -\mathbf{x}_c^{1,3} \cdot \nu_2\, \check{p} \quad \Longrightarrow \quad \check{q} = \gamma\, \check{p},$$

for some $\gamma \neq 0$. We return to the reduced condition, which is now seen to be

$$\big[(\mathbf{x} - \mathbf{x}_c^{1,3})\, \mathbf{x} \cdot \nu_2 + \gamma(\mathbf{x} - \mathbf{x}_c^{2,4})\, \mathbf{x} \cdot \nu_1\big]\check{p} = \mathbf{x}\, r$$

or

$$\mathbf{x}[\mathbf{x} \cdot \nu_2 + \gamma\mathbf{x} \cdot \nu_1]\check{p} - [\mathbf{x}_c^{1,3}\, \mathbf{x} \cdot \nu_2 + \gamma\mathbf{x}_c^{2,4}\, \mathbf{x} \cdot \nu_1]\check{p} = \mathbf{x}\, r.$$

The right-hand side is in $\tilde{\mathbb{P}}_{k-1}$, $k \geq 3$, so there can be no net lower order terms on the left. There are no terms of order 0. Terms of order 1 would appear if $\check{p}$ had terms of order 0, so we see that $\check{p}$ has no terms of order 0. We continue to terms of order $2, 3, \ldots, k-2$ and conclude that $\check{p} = 0$, since it is in $\mathbb{P}_{k-3}$. This shows that $p = q = r = 0$ is the only possibility, and thus the space $\breve{\mathbb{B}}_k$ contains all the bubbles.

Finally, the supplemental vectors $\mathbb{S}_k$ are combined with vectors from $\breve{\mathbb{E}}_k$ to remove the normal components, creating the local space $\breve{\mathbb{S}}_k$. Then we have constructed explicitly a shape function basis for the decomposition

$$\mathbf{V}_{\mathrm{AC}}^k(E) = \breve{\mathbb{E}}_k \oplus \breve{\mathbb{B}}_k \oplus \breve{\mathbb{S}}_k. \tag{5.9}$$

The bubbles and supplementary shape functions are entirely local and therefore easy to implement, and the edge shape functions are easy to pair across element edges.

The reduced $H(\mathrm{div})$-approximating space $\mathbf{V}_{\mathrm{AC}}^{k,\mathrm{red}}$ is not as simple to implement, since we do not have all of the easily constructible edge and bubble shape functions. Using what we have, we note that the Helmholtz-like decomposition (2.1) implies that

$$\begin{aligned}\mathbf{V}_{\mathrm{AC}}^{k,\mathrm{red}}(E) = \mathbb{P}_k^2 \oplus \mathbb{S}_k &= \mathbb{P}_{k-1} \oplus \mathbf{x}\tilde{\mathbb{P}}_{k-1} \oplus \operatorname{curl} \tilde{\mathbb{P}}_{k+1} \oplus \mathbb{S}_k \\ &= \breve{\mathbb{E}}_{k-1} \oplus \breve{\mathbb{B}}_{k-1} \oplus \operatorname{curl} \tilde{\mathbb{P}}_{k+1} \oplus \mathbb{S}_k,\end{aligned}$$

so we require a decomposition of the form

$$\mathbf{V}_{\mathrm{AC}}^{k,\mathrm{red}}(E) = \breve{\mathbb{E}}_{k-1} \oplus \breve{\mathbb{B}}_{k-1} \oplus \tilde{\breve{\mathbb{E}}}_k \oplus \tilde{\breve{\mathbb{B}}}_k, \tag{5.10}$$

where $\tilde{\breve{\mathbb{E}}}_k \oplus \tilde{\breve{\mathbb{B}}}_k$ contains the vectors $\operatorname{curl} \tilde{\mathbb{P}}_{k+1} \oplus \mathbb{S}_k$ and consists of the highest order edge basis vectors and additional bubbles. As we saw in the proof of unisolvence, the space $\mathbb{S}_k$ is necessary to construct a basis for $\mathbf{V}_{\mathrm{AC}}^{k,\mathrm{red}}(E)$ that respects the edge and divergence DOFs independently, so we need to include $\mathbb{S}_k$ in the construction of $\tilde{\breve{\mathbb{E}}}_k$ (since the divergences of $\mathbb{S}_k$ vanish). We construct the edge basis $\breve{\mathbb{E}}_{k-1}$ up to order $k-1$ as above, and then we construct the edge basis for polynomials in $\tilde{\mathbb{P}}_k(e)$ on each edge e using the vectors defined in (4.24) and (4.26) ($\mathbf{v}_H^k$ and $\mathbf{v}_V^k$) as well as $\mathbb{S}_k$. Removing the low order terms as in (4.41) is possible since we have explicitly formed $\breve{\mathbb{E}}_{k-1}$. Finally, we need to form the rest of the bubbles $\tilde{\breve{\mathbb{B}}}_k$, which are given, e.g., by constructing $\operatorname{curl}(\lambda_H^m \lambda_V^n)$, where $m+n = k+1$ and $m, n > 0$, and then removing the edge DOFs using $\breve{\mathbb{E}}_{k-1} \oplus \tilde{\breve{\mathbb{E}}}_k$.

5.2. Quadrature. It appears that general quadrature rules on a general quadrilateral E are not available for approximate integration over E. Nevertheless, there are at least two simple ways to develop and apply an accurate quadrature rule. The simplest to describe is to use a high order quadrature rule defined on a triangle (which are known to exist), and treat the quadrilateral E as the union of two nonoverlapping triangles. This approach may not be the simplest to implement, however. The other approach, which we take in our numerical examples later, is to use a bilinear (not Piola!) mapping of the quadrilateral E to the reference square $\hat{E}$, and then to use a high order tensor-product Gauss rule there, taking into account the Jacobian of the transformation.

6. Some numerical results. In this section we present convergence studies for the full and reduced AC spaces and the corresponding RT and BDM spaces. The test problem is defined on the unit square $\Omega = (0,1)^2$ with the coefficient $a = 1$ and the source function $f(\mathbf{x}) = 2\pi^2 \sin(\pi x)\sin(\pi y)$. The exact solution is

$$p(x,y) = \sin(\pi x)\sin(\pi y) \quad \text{and} \quad \mathbf{u}(x,y) = -\pi \begin{pmatrix} \cos(\pi x)\sin(\pi y) \\ \sin(\pi x)\cos(\pi y) \end{pmatrix}.$$

In the computations, we consider a mixed boundary condition. On p we impose a homogeneous Dirichlet condition on the left boundary, and on $\mathbf{u}\cdot\nu$ we impose a nonhomogeneous Neumann condition on the rest of the boundary. The finite element solutions were computed by adopting two different sequences of meshes. The first is a uniform mesh of n^2 square elements and the second is a mesh of n^2 trapezoids of base h and parallel vertical edges of size $0.75h$ and $1.25h$, as proposed in [3] and shown in Figure 2.

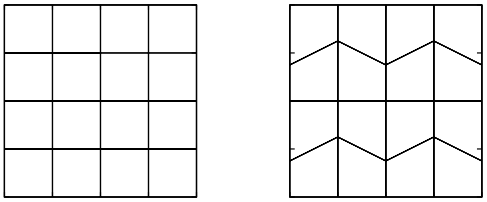

FIG. 2. *Mesh of* 4×4 *squares on the left and trapezoids on the right.*

TABLE 2
Errors and orders of convergence for RT_0 *and* AC_0.

		$\|p - p_h\|$		$\|\mathbf{u} - \mathbf{u}_h\|$		$\|\nabla \cdot (\mathbf{u} - \mathbf{u}_h)\|$	
n	DOF	Error	Order	Error	Order	Error	Order
RT_0 and AC_0 on square meshes							
4	56	1.58e-01		5.13e-01		3.09e-00	
8	208	8.00e-02	0.99	2.53e-01	1.02	1.57e-00	0.98
16	800	4.01e-02	1.00	1.26e-01	1.01	7.90e-01	0.99
32	3136	2.00e-02	1.00	6.30e-02	1.00	3.95e-01	1.00
RT_0 on trapezoidal meshes							
4	56	1.62e-01		5.52e-01		3.45e-00	
8	208	8.23e-02	0.98	2.75e-01	1.00	2.16e-00	0.68
16	800	4.13e-02	1.00	1.38e-01	1.00	1.66e-00	0.38
32	3136	2.07e-02	1.00	6.89e-02	1.00	1.51e-00	0.14
AC_0 on trapezoidal meshes							
4	56	1.62e-01		5.47e-01		3.16e-00	
8	208	8.19e-02	0.98	2.70e-01	1.02	1.61e-00	0.97
16	800	4.11e-02	1.00	1.35e-01	1.00	8.10e-01	0.99
32	3136	2.05e-02	1.00	6.74e-02	1.00	4.06e-01	1.00

6.1. Full $H(\mathrm{div})$-approximation spaces. In Table 2 we present the errors and the orders of convergence for the lowest index full $H(\mathrm{div})$-approximation spaces RT_0 and AC_0. The second column of the table indicates the total DOFs of the problem, that is, the number of equations of the linear system originated by the saddle point problem. It is important to note that in some cases this total dimension can be reduced by special implementation techniques, such as the condensation of local degrees of freedom. On a rectangular mesh, RT_0 and AC_0 are the same space and give first order approximation of the scalar p, the vector $\mathbf{u}$, and the divergence $\nabla \cdot \mathbf{u}$. As expected, on trapezoidal meshes, RT_0 retains first order approximation of the scalar and the vector but loses convergence of the divergence, while AC_0 shows first order for all three quantities.

The results for RT_1 and AC_1 (which are different spaces even on rectangular meshes) are shown in Table 3. Second order convergence is obtained for all the approximations on rectangular meshes, and the errors for RT_1 are slightly smaller than for AC_1, but at the expense of more degrees of freedom. On trapezoidal meshes, AC_1 gives second order approximation of all quantities, whereas RT_1 shows second order only for the scalar and vector variables, and the divergence reduces to first order of convergence.

The same pattern is seen for RT_2 and AC_2 in Table 4. Third order approximation is achieved by AC_2 on all the meshes for all the quantities. We see the same convergence rates for RT_2 except that the divergence on trapezoidal meshes is only second order.

TABLE 3
Errors and orders of convergence for RT_1 *and* AC_1.

		$\|p-p_h\|$		$\|\mathbf{u}-\mathbf{u}_h\|$		$\|\nabla\cdot(\mathbf{u}-\mathbf{u}_h)\|$	
n	DOF	Error	Order	Error	Order	Error	Order
RT_1 on square meshes							
4	208	1.61e-02		5.10e-02		3.18e-01	
8	800	4.05e-03	1.99	1.28e-02	2.00	8.00e-02	1.99
16	3136	1.02e-03	2.00	3.19e-03	2.00	2.00e-02	2.00
32	12416	2.54e-04	2.00	7.98e-04	2.00	5.01e-03	2.00
AC_1 on square meshes							
4	160	2.97e-02		5.45e-02		5.86e-01	
8	608	7.56e-03	1.97	1.29e-02	2.08	1.49e-01	1.97
16	2368	1.90e-03	1.99	3.20e-03	2.01	3.75e-02	1.99
32	9344	4.75e-04	2.00	7.98e-04	2.00	9.38e-03	2.00
RT_1 on trapezoidal meshes							
4	208	1.87e-02		5.48e-02		4.77e-01	
8	800	4.73e-03	1.99	1.36e-02	2.01	1.79e-01	1.42
16	3136	1.18e-03	2.00	3.39e-03	2.00	7.99e-02	1.16
32	12416	2.96e-04	2.00	8.46e-04	2.00	3.87e-02	1.05
AC_1 on trapezoidal meshes							
4	160	3.08e-02		6.40e-02		6.07e-01	
8	608	7.85e-03	1.97	1.57e-02	2.03	1.55e-01	1.97
16	2368	1.97e-03	1.99	3.91e-03	2.00	3.89e-02	1.99
32	9344	4.94e-04	2.00	9.76e-04	2.00	9.74e-03	2.00

TABLE 4
Errors and orders of convergence for RT_2 *and* AC_2.

		$\|p-p_h\|$		$\|\mathbf{u}-\mathbf{u}_h\|$		$\|\nabla\cdot(\mathbf{u}-\mathbf{u}_h)\|$	
n	DOF	Error	Order	Error	Order	Error	Order
RT_2 on square meshes							
4	456	1.07e-03		3.38e-03		2.11e-02	
8	1776	1.35e-04	2.99	4.23e-04	3.00	2.66e-03	2.99
16	7008	1.69e-05	3.00	5.30e-05	3.00	3.33e-04	3.00
32	27840	2.11e-06	3.00	6.62e-06	3.00	4.16e-05	3.00
AC_2 on square meshes							
4	296	3.76e-03		4.07e-03		7.41e-02	
8	1136	4.77e-04	2.98	4.42e-04	2.98	9.42e-03	2.98
16	4448	5.99e-05	2.99	5.35e-05	2.99	1.18e-03	2.99
32	17600	7.50e-06	3.00	6.64e-06	3.00	1.48e-04	3.00
RT_2 on trapezoidal meshes							
4	456	1.49e-03		4.10e-03		4.61e-02	
8	1776	1.88e-04	2.99	5.13e-04	3.00	9.70e-03	2.25
16	7008	2.35e-05	3.00	6.41e-05	3.00	2.29e-03	2.08
32	27840	2.94e-06	3.00	8.01e-06	3.00	5.65e-04	2.02
AC_2 on trapezoidal meshes							
4	296	4.09e-03		8.57e-03		8.05e-02	
8	1136	5.20e-04	2.97	1.07e-03	3.00	1.03e-02	2.97
16	4448	6.53e-05	2.99	1.35e-04	3.00	1.29e-03	3.00
32	17600	8.18e-06	3.00	1.68e-05	3.00	1.61e-04	3.00

6.2. Reduced H(div)-approximation spaces. The results for the reduced H(div)-approximation spaces BDM_k and AC_k^{red} for $k = 1$ and 2 are shown in Tables 5 and 6, respectively. These spaces have the same dimension, and they coincide on rectangular meshes. As predicted, they give order $k+1$ approximation for the vector $\mathbf{u}$ and order k for the scalar p and the divergence $\nabla\cdot\mathbf{u}$ on rectangular meshes.

TABLE 5
Errors and orders of convergence for BDM_1 *and* $\mathrm{AC}_1^{\mathrm{red}}$.

		$\|p-p_h\|$		$\|\mathbf{u}-\mathbf{u}_h\|$		$\|\nabla\cdot(\mathbf{u}-\mathbf{u}_h)\|$	
n	DOF	Error	Order	Error	Order	Error	Order
BDM_1 and $\mathrm{AC}_1^{\mathrm{red}}$ on square meshes							
4	96	1.64e-01		2.45e-01		3.09e-00	
8	352	8.07e-02	1.02	6.32e-02	1.96	1.57e-00	0.98
16	1344	4.02e-02	1.01	1.59e-02	1.99	7.90e-01	0.99
32	5248	2.01e-02	1.00	3.99e-03	2.00	3.95e-01	1.00
BDM_1 on trapezoidal meshes							
4	96	1.68e-01		2.72e-01		3.45e-00	
8	352	8.30e-02	1.01	7.82e-02	1.80	2.16e-00	0.68
16	1344	4.14e-02	1.01	2.60e-02	1.59	1.66e-00	0.38
32	5248	2.07e-02	1.00	1.07e-02	1.28	1.51e-00	0.14
$\mathrm{AC}_1^{\mathrm{red}}$ on trapezoidal meshes							
4	96	1.67e-01		2.64e-01		3.16e-00	
8	352	8.26e-02	1.01	6.83e-02	1.95	1.61e-00	0.97
16	1344	4.12e-02	1.01	1.72e-02	1.99	8.10e-01	0.99
32	5248	2.06e-02	1.00	4.32e-03	2.00	4.06e-01	1.00

TABLE 6
Errors and orders of convergence for BDM_2 *and* $\mathrm{AC}_2^{\mathrm{red}}$.

		$\|p-p_h\|$		$\|\mathbf{u}-\mathbf{u}_h\|$		$\|\nabla\cdot(\mathbf{u}-\mathbf{u}_h)\|$	
n	DOF	Error	Order	Error	Order	Error	Order
BDM_2 and $\mathrm{AC}_2^{\mathrm{red}}$ on square meshes							
4	200	2.97e-02		2.31e-02		5.86e-01	
8	752	7.56e-03	1.97	2.52e-03	3.19	1.49e-01	1.97
16	2912	1.90e-03	1.99	2.91e-04	3.11	3.75e-02	1.99
32	11454	4.75e-04	2.00	3.50e-05	3.06	9.38e-03	2.00
BDM_2 on trapezoidal meshes							
4	200	3.53e-02		5.83e-02		9.29e-01	
8	752	1.14e-02	1.63	1.50e-02	1.95	3.90e-01	1.25
16	2912	4.55e-03	1.33	4.39e-03	1.78	1.84e-01	1.08
32	11454	2.11e-03	1.11	1.54e-03	1.51	9.06e-02	1.02
$\mathrm{AC}_2^{\mathrm{red}}$ on trapezoidal meshes							
4	200	3.08e-02		2.74e-02		6.07e-01	
8	752	7.85e-03	1.97	3.26e-03	3.07	1.55e-01	1.97
16	2912	1.97e-03	1.99	3.95e-04	3.05	3.89e-02	1.99
32	11454	4.94e-04	2.00	4.85e-05	3.03	9.74e-03	2.00

On trapezoidal meshes, when BDM_k is used, the results indicate that the order of convergence of the divergence is only $k-1$. In this case, the poor approximation of the divergence also affects the order of convergence of the vector and scalar variables, degrading the original orders (which is also predicted and explained by the theory of Arnold, Boffi, and Falk [3]). When $\mathrm{AC}_k^{\mathrm{red}}$ is used instead, the orders of convergence on the rectangular meshes are achieved for trapezoids, i.e., $k+1$ approximation for the vector $\mathbf{u}$ and order k for the scalar p and the divergence $\nabla\cdot\mathbf{u}$.

7. Concluding remarks. We developed the AC spaces, two families of mixed finite elements for quadrilateral meshes that are uniformly inf-sup stable, achieve optimal rates of convergence, and have minimal dimension. The key theoretical result was a Helmholtz-like decomposition of vector polynomials (Theorem 2.1). Our idea was to construct the element basis functions directly over the elements and then to supplement the space locally by two (or one, when $k=0$) basis functions that are

Piola mapped, so that we could prove existence of, and actually construct, the π-projection operator. We used standard local coordinates with origin at the midpoints of the edges and the element, rather than, e.g., generalized barycentric coordinates (see [25]).

One family has full $H(\mathrm{div})$-approximation and the other has reduced $H(\mathrm{div})$-approximation. The two families are identical except for inclusion of a minimal set of vector and scalar polynomials needed for higher order approximation of $\nabla \cdot \mathbf{u}$ and p, and so in some sense we clarified and unified the treatment of finite element approximation between the two classes of mixed spaces.

We also developed an implementable local basis for the AC spaces, and we presented numerical results that confirm the convergence theory.

The analogue of our spaces on triangles is the classical RT and BDM spaces, since these have minimal dimension for full and reduced $H(\mathrm{div})$-approximation. Therefore, the AC spaces can be seen as a proper (i.e., lowest dimension) extension of RT and BDM on triangles to quadrilaterals. We expect that our ideas could be extended to elements that are convex polygons with more than four edges. We also expect that $H(\mathrm{curl})$ finite elements could be developed by rotation by 90 degrees.

For three-dimensional domains, it should be clear that we can define prismatic-like finite elements on $E \times I$, where E is a quadrilateral and I is an interval, using AC spaces on E and extending to the third dimension in the usual way; see [16]. It is unclear if we can define similar AC spaces on general hexahedral meshes, since the faces of the elements need not be contained within a plane (the four corners need not be coplanar). If we restrict to hexahedral meshes of elements with planar faces, we believe that similar AC elements can be defined as a generalization of the Arnold–Awanou elements on cubes [1] (see also [21]). We are exploring these issues and expect that the finite element exterior calculus [5, 2] might prove useful.

REFERENCES

[1] D. N. Arnold and G. Awanou, *Finite element differential forms on cubical meshes*, Math. Comp., 83 (2014), pp. 1551–1570.

[2] D. N. Arnold, D. Boffi, and F. Bonizzoni, *Finite element differential forms on curvilinear cubic meshes and their approximation properties*, Numer. Math., 129 (2015), pp. 1–20.

[3] D. N. Arnold, D. Boffi, and R. S. Falk, *Quadrilateral H(div) finite elements*, SIAM. J. Numer. Anal., 42 (2005), pp. 2429–2451.

[4] D. N. Arnold and F. Brezzi, *Mixed and nonconforming finite element methods: Implementation, postprocessing and error estimates*, RAIRO Modél. Math. Anal. Numér., 19 (1985), pp. 7–32.

[5] D. N. Arnold, R. S. Falk, and R. Winther, *Finite element exterior calculus: from Hodge theory to numerical stability*, Bull. Amer. Math. Soc. (N.S.), 47 (2010), pp. 281–354.

[6] D. N. Arnold, L. R. Scott, and M. Vogelius, *Regular inversion of the divergence operator with Dirichlet boundary conditions on a polygon*, Ann. Sc. Norm. Super. Pisa Cl. Sci. (5), 15 (1988), pp. 169–192.

[7] I. Babuška, *The finite element method with Lagrangian multipliers*, Numer. Math., 20 (1973), pp. 179–192.

[8] P. B. Bochev and D. Ridzal, *Rehabilitation of the lowest-order Raviart–Thomas element on quadrilateral grids*, SIAM J. Numer. Anal., 47 (2008), pp. 487–507.

[9] D. Boffi, F. Brezzi, and M. Fortin, *Mixed Finite Element Methods and Applications*, Springer Ser. Comput. Math. 44, Springer, Heidelberg, 2013.

[10] D. Boffi, F. Kikuchi, and J. Schöberl, *Edge element computation of Maxwell's eigenvalues on general quadrilateral meshes*, Math. Models Methods Appl. Sci., 16 (2006), pp. 265–273.

[11] J. H. Bramble and S. R. Hilbert, *Estimation of linear functionals on Sobolev spaces with applications to Fourier transforms and spline interpolation*, SIAM J. Numer. Anal., 7 (1970), pp. 112–124.

[12] S. C. Brenner and L. R. Scott, *The Mathematical Theory of Finite Element Methods*, Springer-Verlag, New York, 1994.
[13] F. Brezzi, *On the existence, uniqueness and approximation of saddle-point problems arising from Lagrangian multipliers*, RAIRO, 8 (1974), pp. 129–151.
[14] F. Brezzi, J. Douglas, Jr., and L. D. Marini, *Two families of mixed elements for second order elliptic problems*, Numer. Math., 47 (1985), pp. 217–235.
[15] F. Brezzi and M. Fortin, *Mixed and Hybrid Finite Element Methods*, Springer-Verlag, New York, 1991.
[16] Z. Chen and J. Douglas, Jr., *Prismatic mixed finite elements for second order elliptic problems*, Calcolo, 26 (1989), pp. 135–148.
[17] P. G. Ciarlet, *The Finite Element Method for Elliptic Problems*, North-Holland, Amsterdam, 1978.
[18] M. R. Correa and A. F. D. Loula, *Unconditionally stable mixed finite element methods for Darcy flow*, Comput. Methods Appl. Mech. Engrg., 197 (2008), pp. 1525–1540.
[19] J. Douglas, Jr. and J. E. Roberts, *Global estimates for mixed methods for second order elliptic equations*, Math. Comp., 44 (1985), pp. 39–52.
[20] T. Dupont and L. R. Scott, *Polynomial approximation of functions in Sobolev space*, Math. Comp., 34 (1980), pp. 441–463.
[21] R. S. Falk, P. Gatto, and P. Monk, *Hexahedral H(div) and H(curl) finite elements*, ESAIM Math. Model. Numer. Anal., 45 (2011), pp. 115–143.
[22] V. Girault and P. A. Raviart, *Finite Element Methods for Navier-Stokes Equations: Theory and Algorithms*, Springer-Verlag, Berlin, 1986.
[23] J. Li, T. Arbogast, and Y. Huang, *Mixed methods using standard conforming finite elements*, Comput. Methods Appl. Mech. Engrg., 198 (2009), pp. 680–692.
[24] J. C. Nédélec, *Mixed finite elements in* $\mathbf{R}^3$, Numer. Math., 35 (1980), pp. 315–341.
[25] A. Rand, A. Gillette, and C. Bajaj, *Quadratic serendipity finite elements on polygons using generalized barycentric coordinates*, Math. Comp., 83 (2014).
[26] R. A. Raviart and J. M. Thomas, *A mixed finite element method for* 2*nd order elliptic problems*, in Mathematical Aspects of Finite Element Methods, I. Galligani and E. Magenes, eds., Lecture Notes in Math. 606, Springer-Verlag, New York, 1977, pp. 292–315.
[27] J. E. Roberts and J.-M. Thomas, *Mixed and hybrid methods*, in Handbook of Numerical Analysis, P. G. Ciarlet and J. L. Lions, eds., Vol. 2, North-Holland, Amsterdam, 1991, pp. 523–639.
[28] J. Shen, *Mixed Finite Element Methods: Analysis and Computational Aspects*, Ph.D. thesis, University of Wyoming, 1992.
[29] J. Shen, *Mixed Finite Element Methods on Distorted Rectangular Grids*, Tech. report ISC-94-13-MATH, Institute for Scientific Computation, Texas A&M University, College Station, 1994.
[30] J. M. Thomas, *Sur l'analyse numerique des methodes d'elements finis hybrides et mixtes*, Ph.D. thesis, Sciences Mathematiques, à l'Universite Pierre et Marie Curie, 1977.